Baryon Acoustic Oscillations

Vicent J. Martínez (Valencia University)

July 18, 2017

Observatori Astronòmic
Vniversitat de València

Vniversitat de València

Outline

0 Introduction. Correlation function and power spectum

1. Physics of Baryon Acoustic Oscillations (BAO)
2. BAO previous detections
3. Detection and Reconstruction of Baryon Acoustic Structures

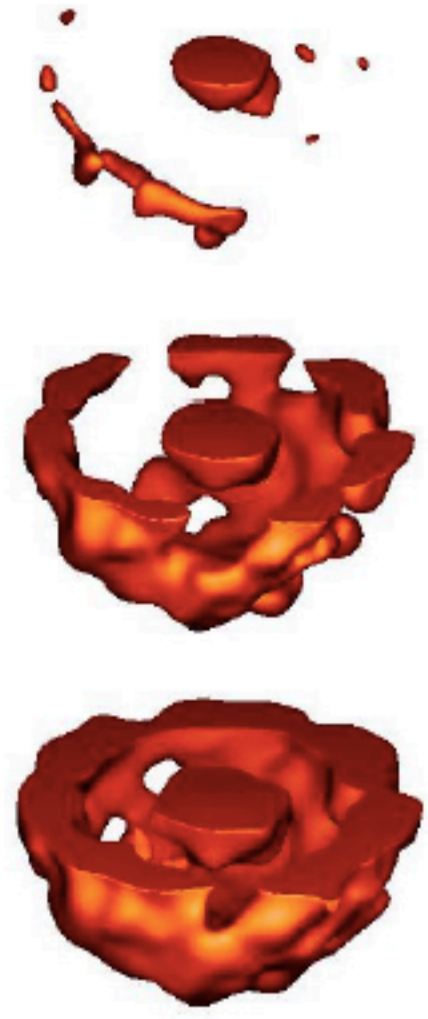

Correlation Analysis

The two-point correlation function

- Infinitesimal interpretation:

$$\boxed{dP_{12} = \bar{n}^2[1 + \xi(\mathbf{r})]dV_1 dV_2}$$

is the joint probability that in each one of the two infinitesimal volumes dV_1 and dV_2, with separation vector $\mathbf{r}$, lies a galaxy.

is the average number density (intensity)

Spatial Correlation Function

Matsubara

- Totsuji & Kihara (1969)
  - Spatial correlation function of galaxies

    Clustering pattern of galaxies, as a function of scales

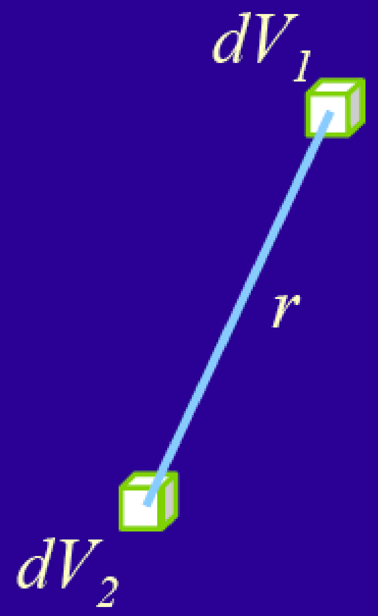

$$dP = \bar{n}^2 dV_1 dV_2 \left[1 + \xi(r)\right]$$

Probability of having galaxies in both cells

Spatial correlation function

Vol. 21, No. 3 Publications of the Astronomical Society of Japan 1969

The Correlation Function for the Distribution of Galaxies

Hiroo TOTSUJI and Taro KIHARA

Department of Physics, Faculty of Science, University of Tokyo

(Received May 15, 1969; revised June 26, 1969)

Abstract

The correlation function for the spatial distribution of galaxies in the universe is determined to be $(r_0/r)^{1.8}$, r being the distance between galaxies. The characteristic length r_0 is 4.7 Mpc. This determination is based on the distribution of galaxies brighter than the apparent magnitude 19 counted by SHANE and WIRTANEN (1967). The reason why the correlation function has the form of inverse power of r is that the universe is in a state of "neutral" stability.

$$\frac{\text{Number of data pairs with separation } r}{\text{Number of random pairs with separation } r} = 1 + \xi(r)$$

Power-law: $\xi(r) = (r_0/r)^{\gamma}$
slope $\gamma = -1.8$

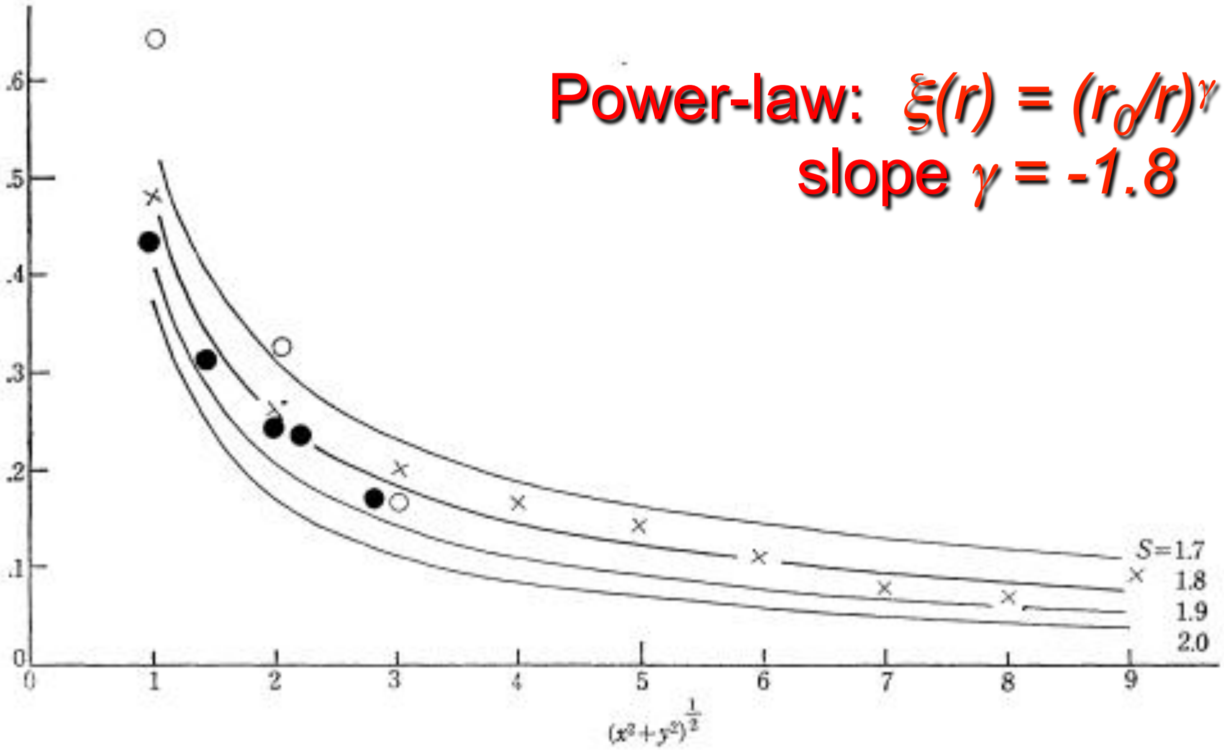

FIG. 2. Comparison of the empirical and theoretical values of $\frac{\langle\{N_1-\langle N\rangle\}\{N_2-\langle N\rangle\}\rangle}{\langle\{N-\langle N\rangle\}^2\rangle-\langle N\rangle}$. The filled circles indicate the empirical values obtained by the authors, and the open circles and crosses by NEYMAN et al.; the unit solid angle is 1°×1° for the circles and 10′×10′ for the crosses. The curves are theoretical values for s=1.7, 1.8, 1.9, and 2.0.

Estimators

Minus estimator

For galaxies close to the boundary the number of neighbors is obviously underestimated. One way to overcome this problem is to consider as centers for counting neighbors only galaxies lying within an inner window $W_{\rm in}$; then we can average

$$\hat{\xi}_{\rm min}(r) = \frac{V(W)}{N N_{\rm in}} \sum_{i=1}^{N_{\rm in}} \frac{n_i(r)}{V_{\rm sh}} - 1,$$

where $V_{\rm sh}$ is the volume of the shell of width dr.

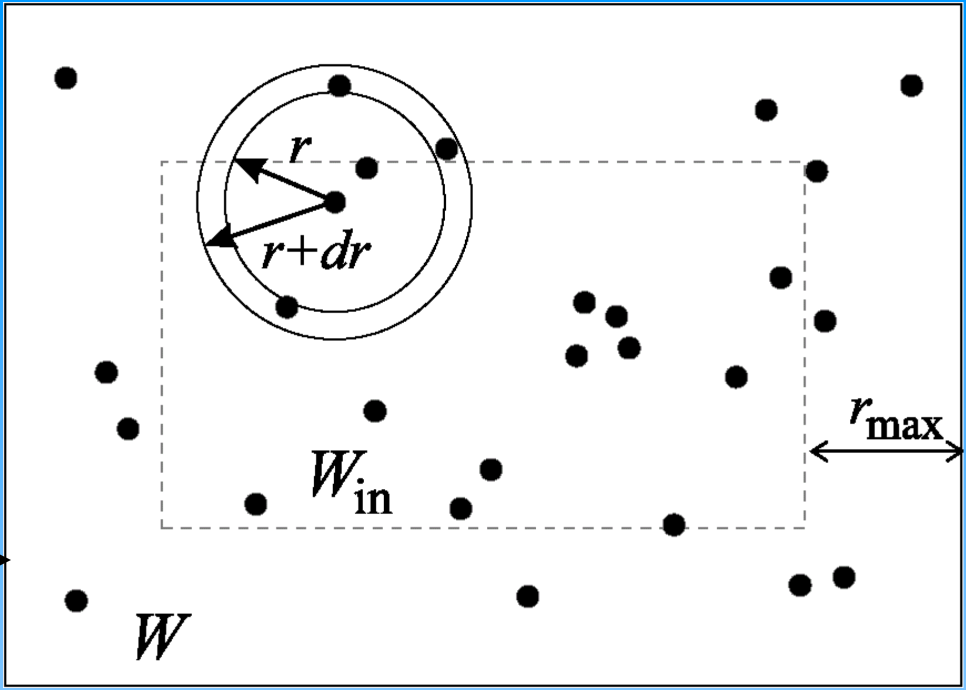

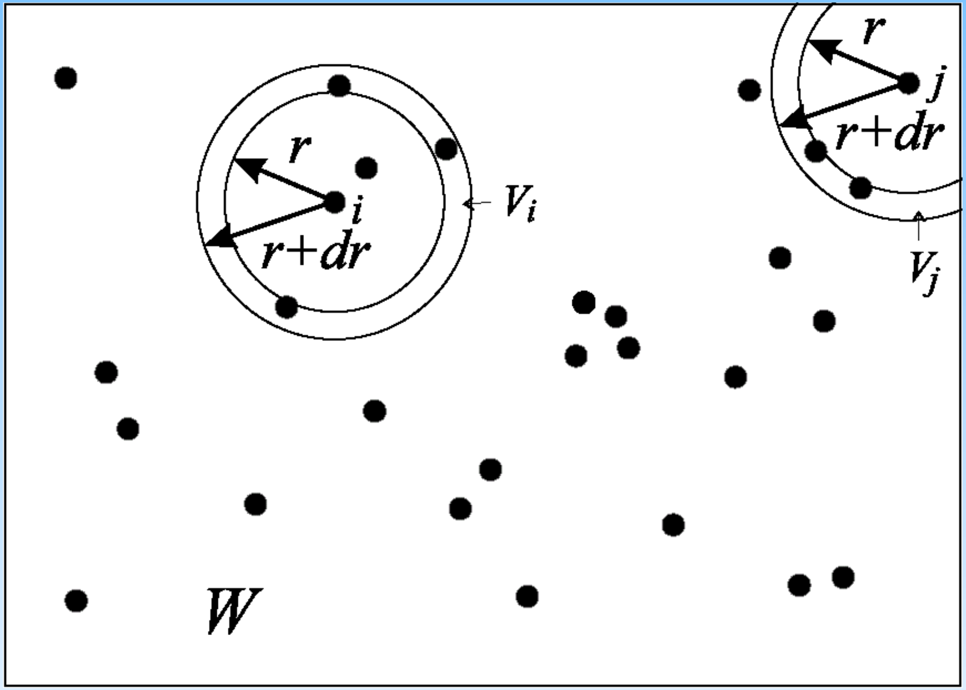

Edge-corrected estimarors

$$\hat{\xi}_{\rm RIV}(r) = \frac{V(W)}{N^2} \sum_{i=1}^{N} \frac{n_i(r)}{V_i} - 1,$$

$n_i(r)$ is the number of neighbors at distance in the interval $[r, r+dr]$ from galaxy i, V_i is the volume of the intersection of the shell with W. When W is a cube, an analytic expression for V_i is provided in Baddeley et al. (1993) *Appl. Statis.*, 42, 641.

$$\xi_N = \frac{N_r(N_r - 1)}{N_d(N_d - 1)} \frac{DD}{RR} - 1$$

$$\xi_{LS} = \frac{\frac{N_r(N_r-1)}{N_d(N_d-1)} DD - \frac{N_r-1}{N_d} DR + RR}{RR}.$$

The Galaxy Correlation Function

- First measured by Totsuji and Kihara, then Peebles et al
- Mostly angular correlations in the beginning
- Later more and more redshift space
- Power law is a good approximation

$$\xi(r) = \left(\frac{r}{r_0}\right)^{-\gamma}$$

- Correlation length r_0=5.4 h^{-1} Mpc
- Exponent is around γ=1.8
- Corresponding angular correlations

$$w(\theta) = \left(\frac{\theta}{\theta_0}\right)^{1-\gamma}$$

(From A. Szalay)

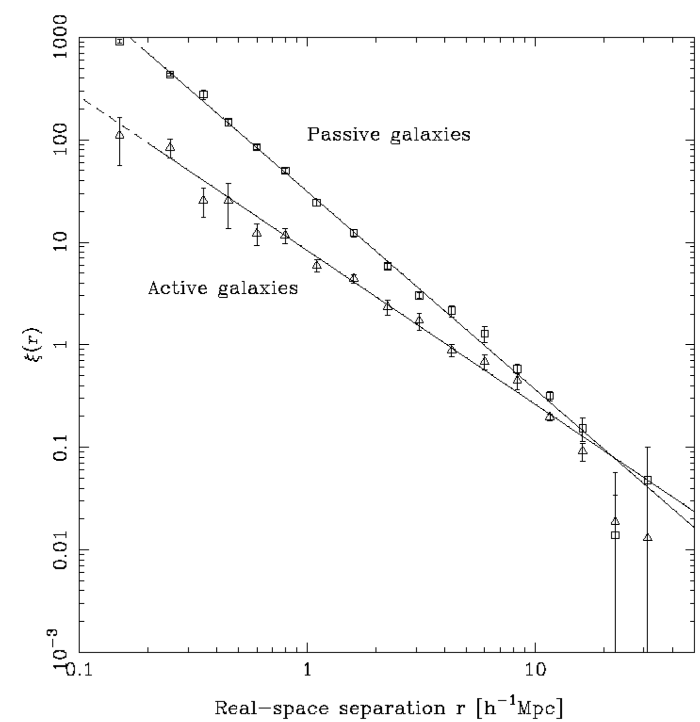

Figure 3. The non-parametric estimates of the real-space correlation functions are shown for both our spectral types, using the method of Saunders, Rowan-Robinson & Lawrence (1992). It can be seen that our assumption of a power law form for $\xi(r)$ is justified out to scales of up to 20 h^{-1} Mpc. The solid lines are the best-fitting power law fits shown in Table 1, whereas the dashed lines are extrapolations of these fits.

Madgwick et al., 2004 (2dFGRS)

Power Spectrum

Quantification of Clustering

Structures in 1-D

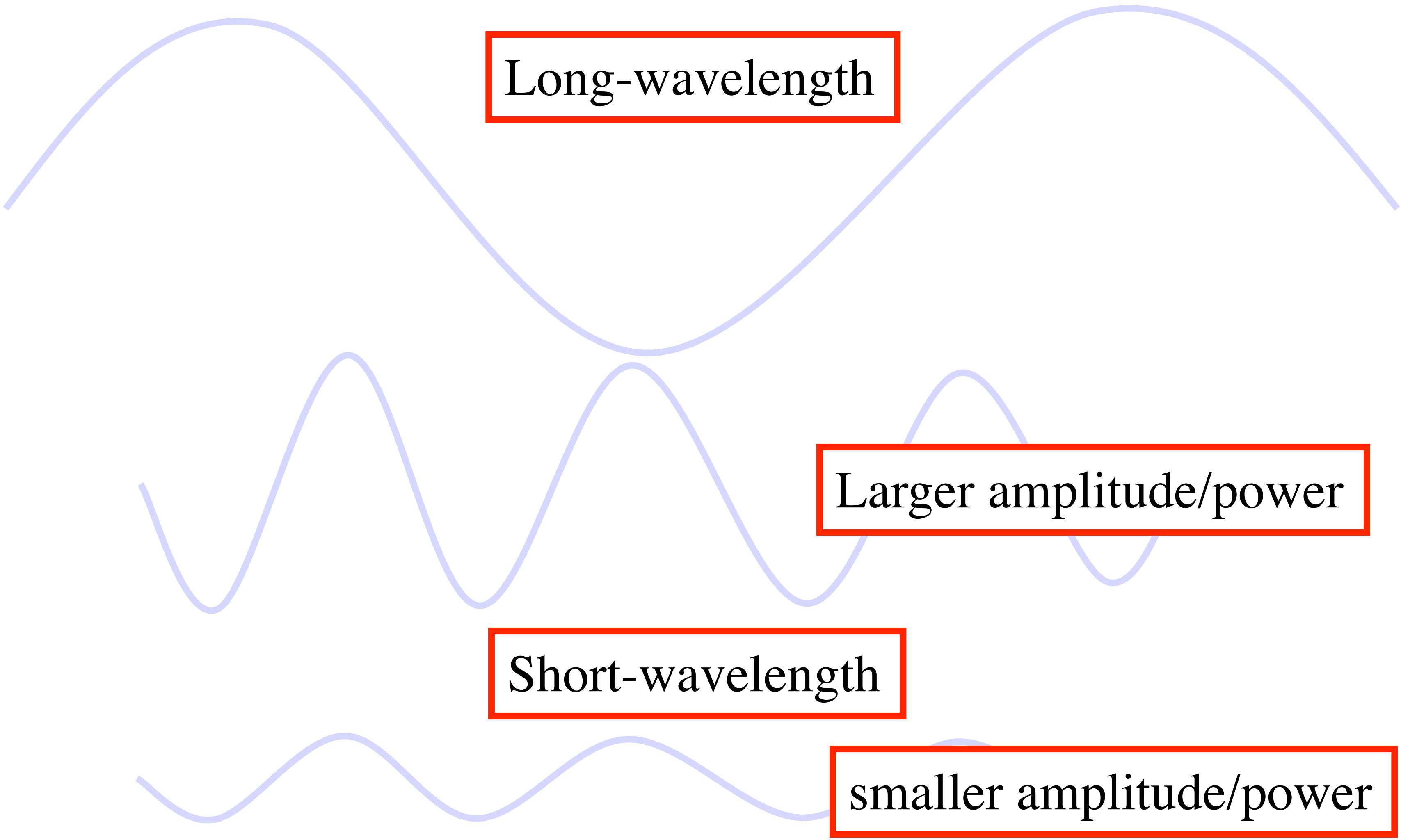

Quantification of Clustering

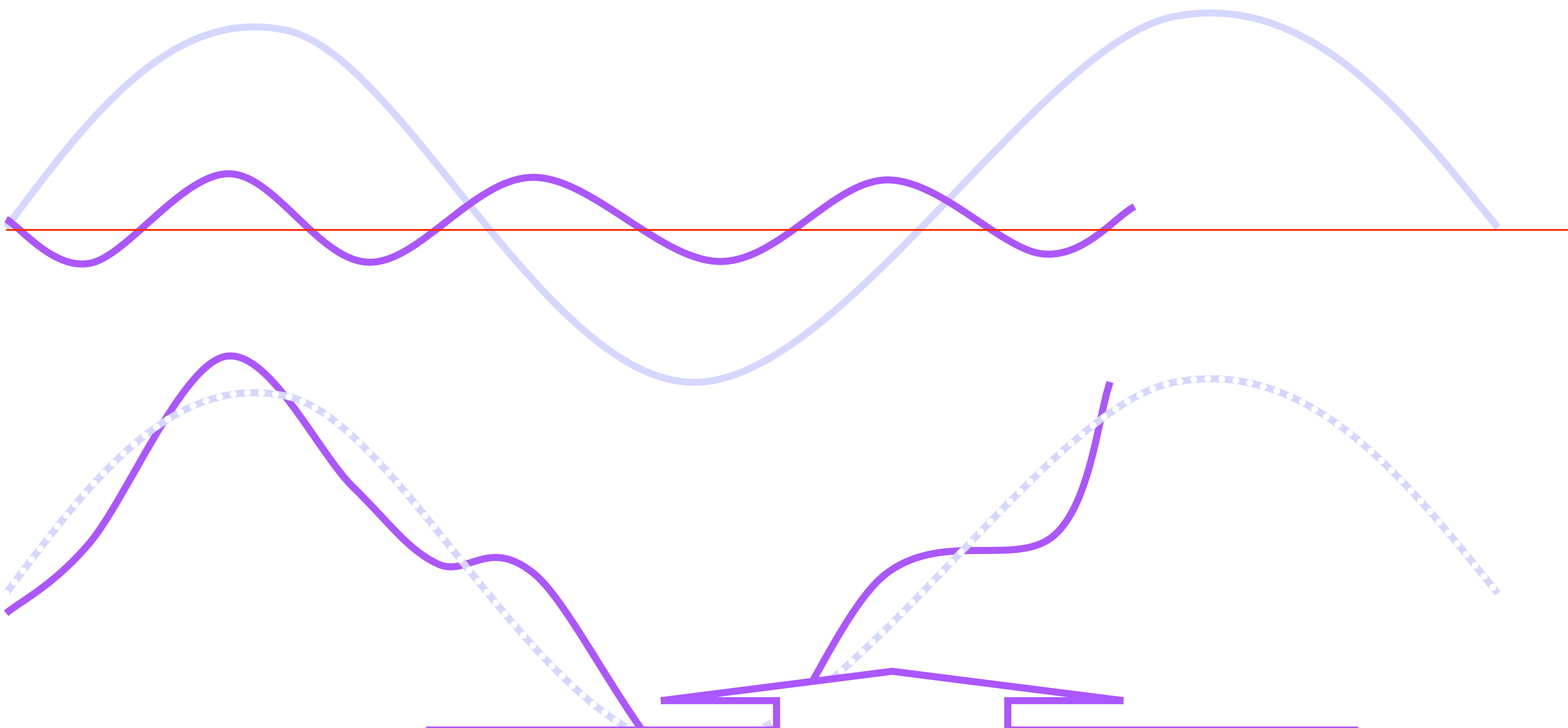

This distribution has a lot of long wavelength power
And a little short wavelength power

Credit: Investigación y Ciencia

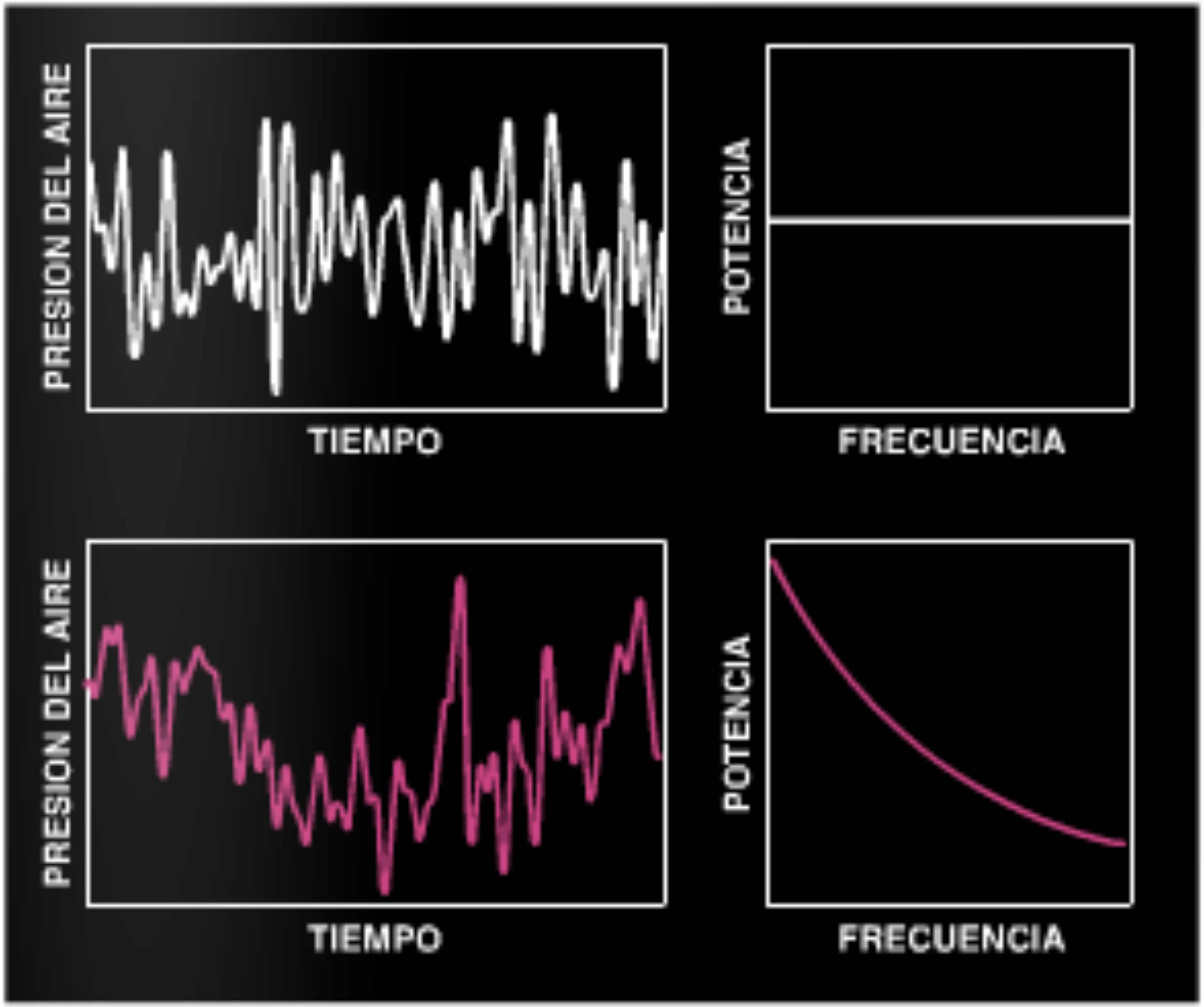

3. LOS RUIDOS BLANCOS Y ROSAS nos rodean. El ruido

Match up the power spectra

from *Sarah Bridle*

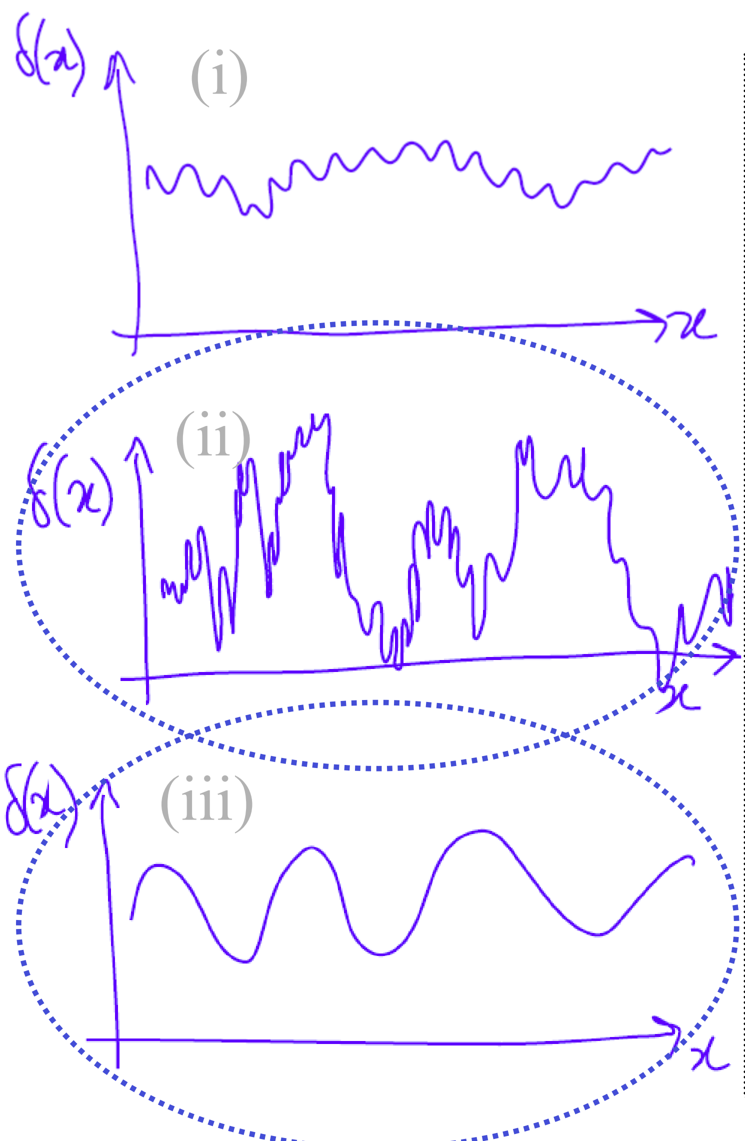

-> C

-> A

-> B

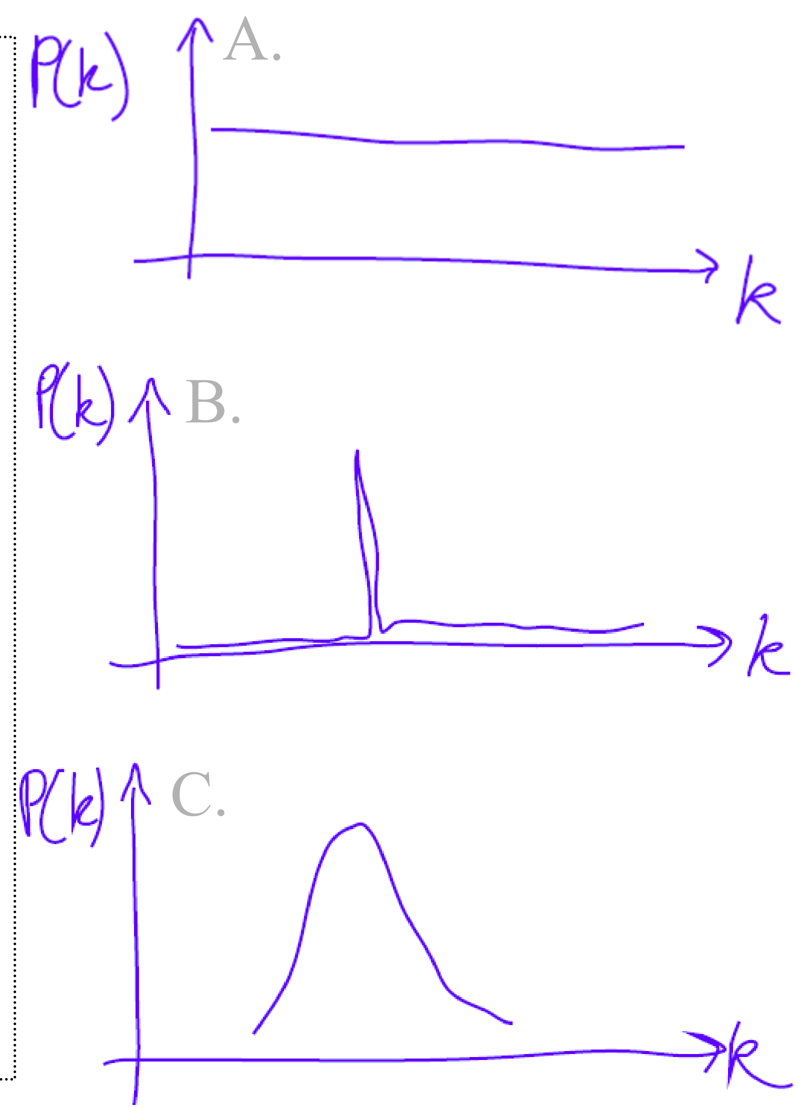

Courtesy of David Kirkby - UC Irvine

The Power Spectrum

- The power spectrum of a function y(x) is:

$$P(\vec{k}) = \left| \frac{1}{\sqrt{2\pi}} \int_{-\infty}^{+\infty} y(\vec{x}) \, \exp(-i\vec{k}\cdot\vec{x}) \, d\vec{x} \right|^2$$
$$= \tilde{y}(\vec{k})\tilde{y}(\vec{k})^*$$

- remember that y(x) is a particular realization of some random field φ(x)

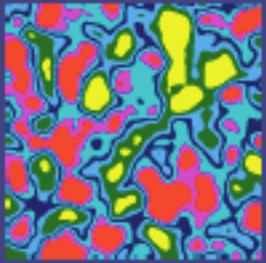

- units are [length]$^{-3}$

Power spectrum

Real space

- Correlation function:

$$\boxed{E\left\{\rho(\mathbf{x})\rho(\mathbf{x}+\mathbf{r})\right\} = \bar{\rho}^2\left[1+\xi(\mathbf{r})\right].}$$

- Density contrast:

$$\delta(\mathbf{x}) = \frac{\rho(\mathbf{x}) - \bar{\rho}}{\bar{\rho}},$$

$$E\left\{\delta(\mathbf{x})\delta(\mathbf{x}+\mathbf{r})\right\} = \xi(\mathbf{r}).$$

Fourier space (advantages)

- It is more intuitive physically, separating processes on different scales.
- Theoretical model predictions are made in terms of power spectrum.
- The amplitudes for different wavenumbers are statistically orthogonal

$$E\left\{\tilde{\delta}(\mathbf{k})\tilde{\delta}^{\star}(\mathbf{k}')\right\} = (2\pi)^3\delta_D(\mathbf{k}-\mathbf{k}')P(\mathbf{k}).$$

is the Fourier amplitude of the overdensity field d at a wavenumber **k**

- Power spectrum — correlation function:

$$P(\mathbf{k}) = \int \xi(\mathbf{r}) e^{i\mathbf{k}\cdot\mathbf{r}}\, d^3r,$$

Fourier transform pair

$$\xi(\mathbf{r}) = \int P(\mathbf{k}) e^{-i\mathbf{k}\cdot\mathbf{r}} \frac{d^3k}{(2\pi)^3},$$

- Isotropy:

$$\xi(r) = 4\pi \int_0^\infty P(k) \frac{\sin(kr)}{kr} \frac{k^2\, dk}{(2\pi)^3}.$$

- Delta-power:

$$\Delta^2(k) = \frac{1}{2\pi^2} P(k) k^3,$$

Physics of baryon acoustic oscillations

(Courtesy of D. Eisenstein)

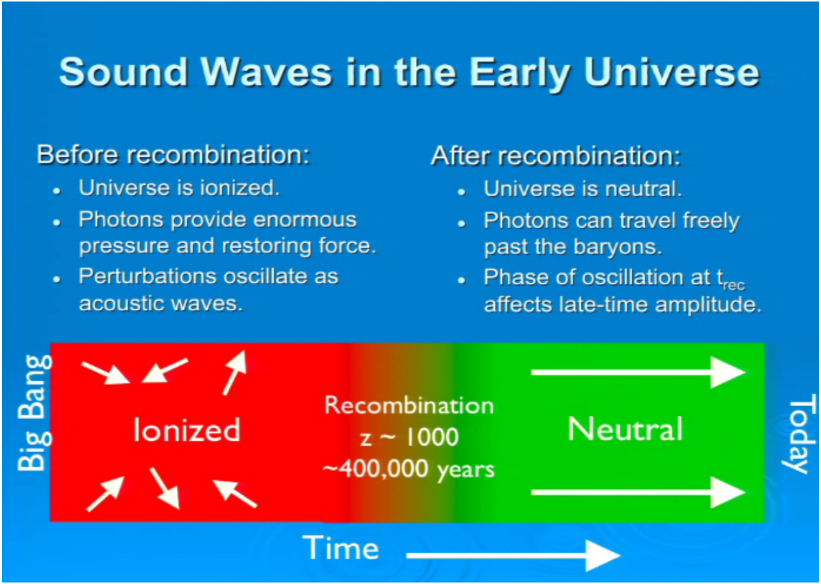

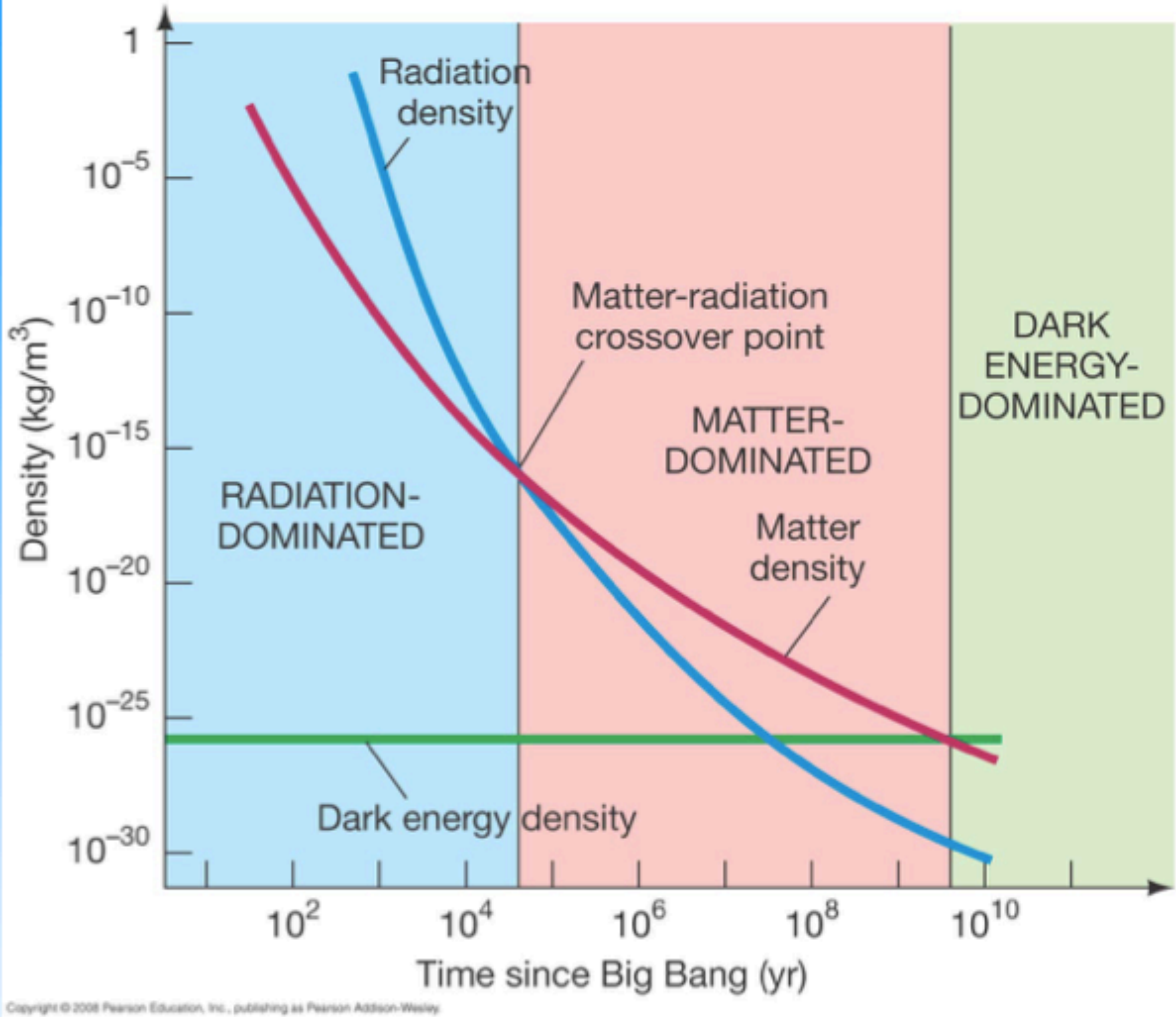

1
10^{-5}
10^{-10}
10^{-15}
10^{-20}
10^{-25}
10^{-30}
Density (kg/m^3)
Radiation density
Matter-radiation crossover point
DARK ENERGY-DOMINATED
MATTER-DOMINATED
RADIATION-DOMINATED
Matter density
Dark energy density
10^2
10^4
10^6
10^8
10^{10}
Time since Big Bang (yr)

Waine Hu web page

http://background.uchicago.edu/~whu/intermediate/gravity.html

Gravity tries to compress the fluid in potential wells.

The photon-baryon fluid is sitting in the gravitational potential wells that are the seeds of structure in the universe. As gravity tries to compress the fluid, radiation pressure resists resulting in acoustic oscillations. Because it acts to resist compression, we will represent the radiation pressure abstractly as springs. Likewise we will represent the inertia of the fluid, or loosely speaking its mass (really energy density), as massive balls falling under gravity:

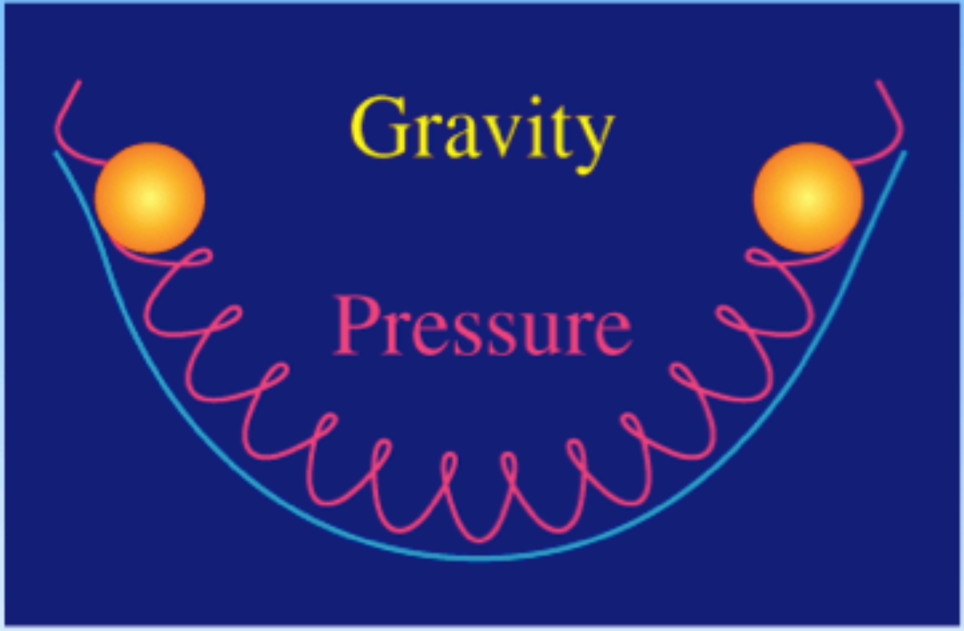

Baryon-photon fluid:

- Sound speed: $c_s = c / \sqrt{3(1+R)}$

$$R = 3\rho_b / 4\rho_\gamma = \delta\rho_b / \delta\rho_\gamma$$

- Before recombination, baryons and radiation form a fluid undergoing acoustic oscillations.
- After decoupling, baryons are free and have nearly no pressure, so they fall to the potential wells of dark matter.

Evolution of matter profile from a central perturbation before recombination

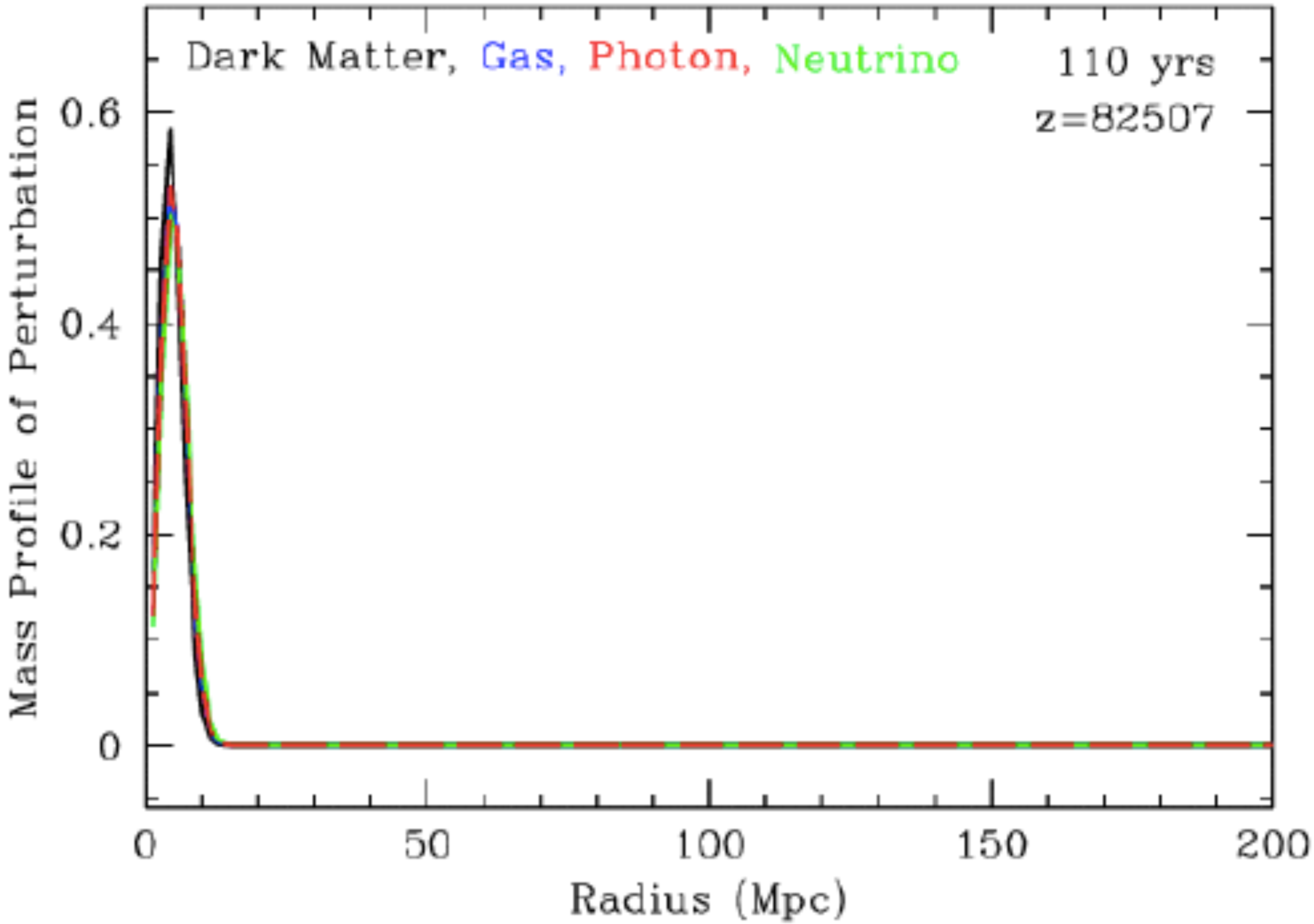

Animation by Daniel Eisenstein

Physics of baryon acoustic oscillations

- Before recombination, baryons and photons are coupled forming a plasma
- Density fluctuations produce sound waves in the plasma
- At recombination ($t \sim 380,000$ years), baryons decouple from photons $\rightarrow$ sound waves become 'frozen'$\rightarrow$ imprint a characteristic 'acoustic' scale in the matter distribution $r_s = \int_0^{t_{\rm rec}} c_s(t)(1+z)\mathrm{d}t \simeq 150\mathrm{Mpc}$

Evolution of matter profile from a central perturbation

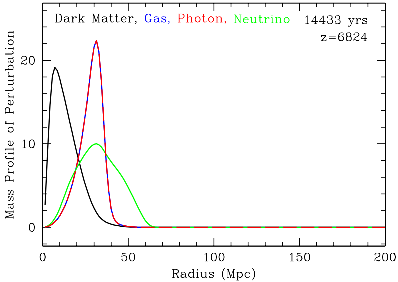

Animation by Daniel Eisenstein

Physics of baryon acoustic oscillations

- Before recombination, baryons and photons are coupled forming a plasma
- Density fluctuations produce sound waves in the plasma
- At recombination ($t \sim 380,000$ years), baryons decouple from photons $\rightarrow$ sound waves become 'frozen'$\rightarrow$ imprint a characteristic 'acoustic' scale in the matter distribution $r_s = \int_0^{t_{\rm rec}} c_s(t)(1+z)\mathrm{d}t \simeq 150\mathrm{Mpc}$

Evolution of matter profile from a central perturbation

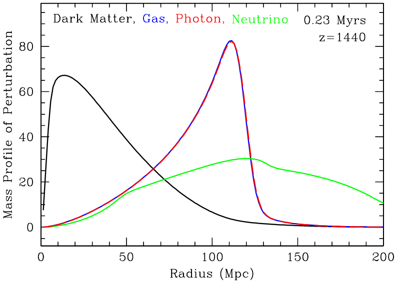

Animation by Daniel Eisenstein

Evolution of matter profile from a central perturbation before recombination

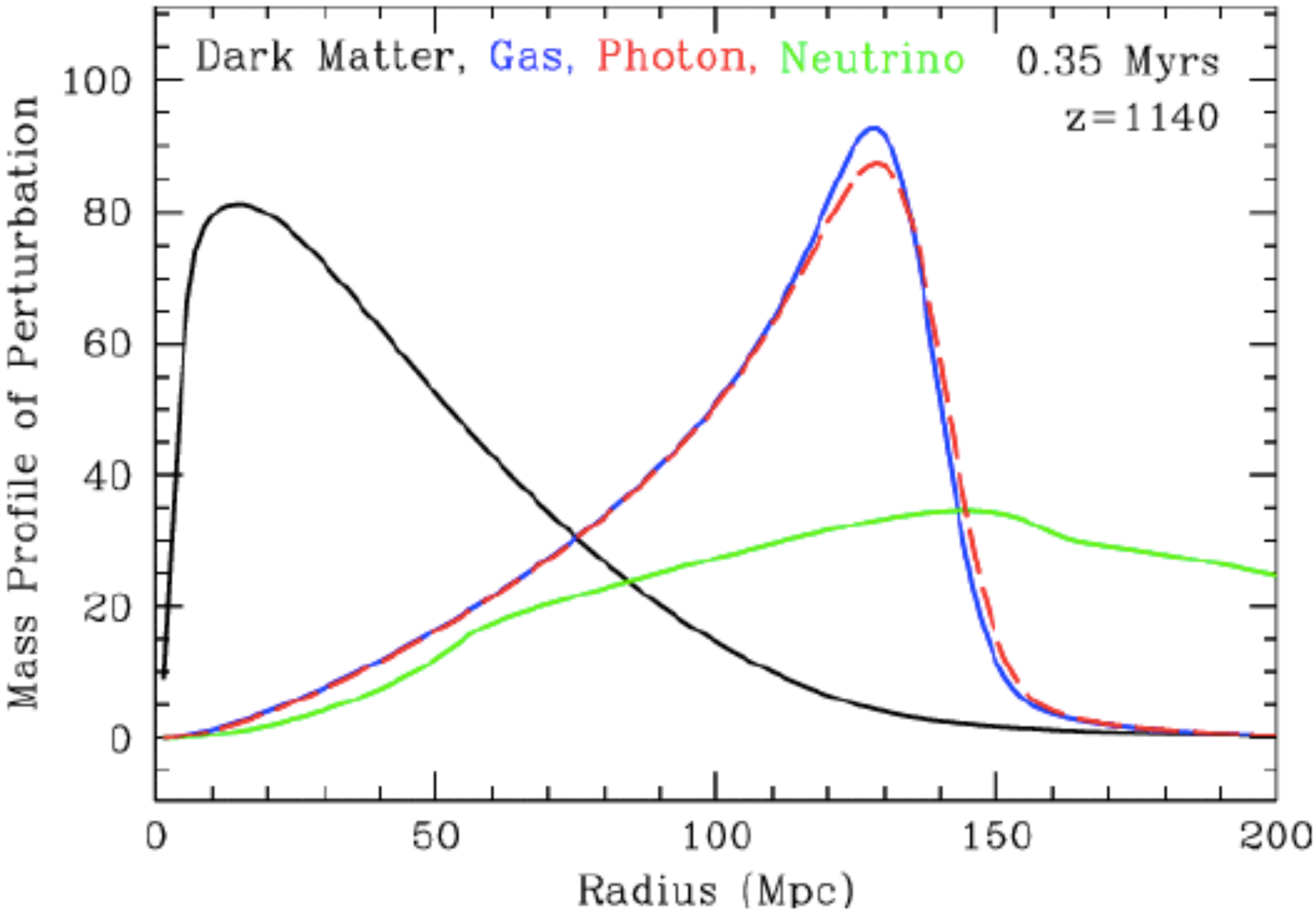

Physics of baryon acoustic oscillations

- Before recombination, baryons and photons are coupled forming a plasma
- Density fluctuations produce sound waves in the plasma
- At recombination ($t \sim 380,000$ years), baryons decouple from photons $\rightarrow$ sound waves become 'frozen' $\rightarrow$ imprint a characteristic 'acoustic' scale in the matter distribution $r_s = \int_0^{t_{\rm rec}} c_s(t)(1+z)\mathrm{d}t \simeq 150\mathrm{Mpc}$

Evolution of matter profile from a central perturbation

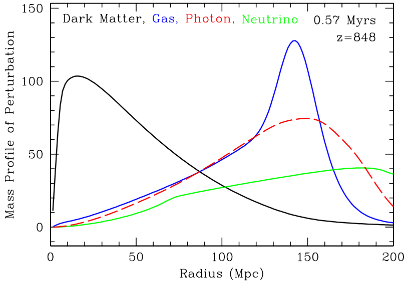

Animation by Daniel Eisenstein

Physics of baryon acoustic oscillations

- Before recombination, baryons and photons are coupled forming a plasma
- Density fluctuations produce sound waves in the plasma

- At recombination ($t \sim 380,000$ years), baryons decouple from photons $\rightarrow$ sound waves become 'frozen'$\rightarrow$ imprint a characteristic 'acoustic' scale in the matter distribution $r_s = \int_0^{t_{\rm rec}} c_s(t)(1+z)\mathrm{d}t \simeq 150\mathrm{Mpc}$

Evolution of matter profile from a central perturbation

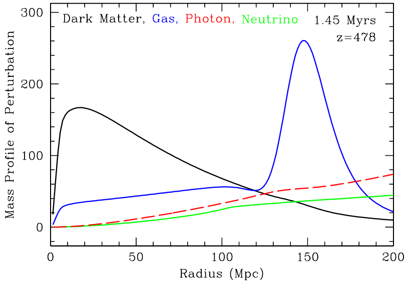

Animation by Daniel Eisenstein

Physics of baryon acoustic oscillations

- Before recombination, baryons and photons are coupled forming a plasma
- Density fluctuations produce sound waves in the plasma

- At recombination ($t \sim 380,000$ years), baryons decouple from photons $\rightarrow$ sound waves become 'frozen'$\rightarrow$ imprint a characteristic 'acoustic' scale in the matter distribution $r_s = \int_0^{t_{\rm rec}} c_s(t)(1+z)\mathrm{d}t \simeq 150\mathrm{Mpc}$

Evolution of matter profile from a central perturbation

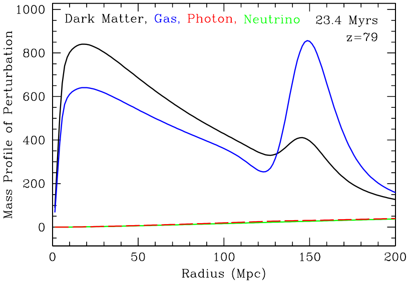

Animation by Daniel Eisenstein

Physics of baryon acoustic oscillations

- Before recombination, baryons and photons are coupled forming a plasma
- Density fluctuations produce sound waves in the plasma
- At recombination ($t \sim 380,000$ years), baryons decouple from photons $\rightarrow$ sound waves become 'frozen'$\rightarrow$ imprint a characteristic 'acoustic' scale in the matter distribution $r_s = \int_0^{t_{\rm rec}} c_s(t)(1+z)\mathrm{d}t \simeq 150\mathrm{Mpc}$

Evolution of matter profile from a central perturbation

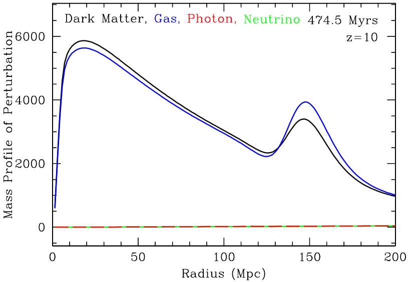

Animation by Daniel Eisenstein

Physics of BAO: Galaxy Distribution

Evolution of matter profile from a central perturbation after recombination

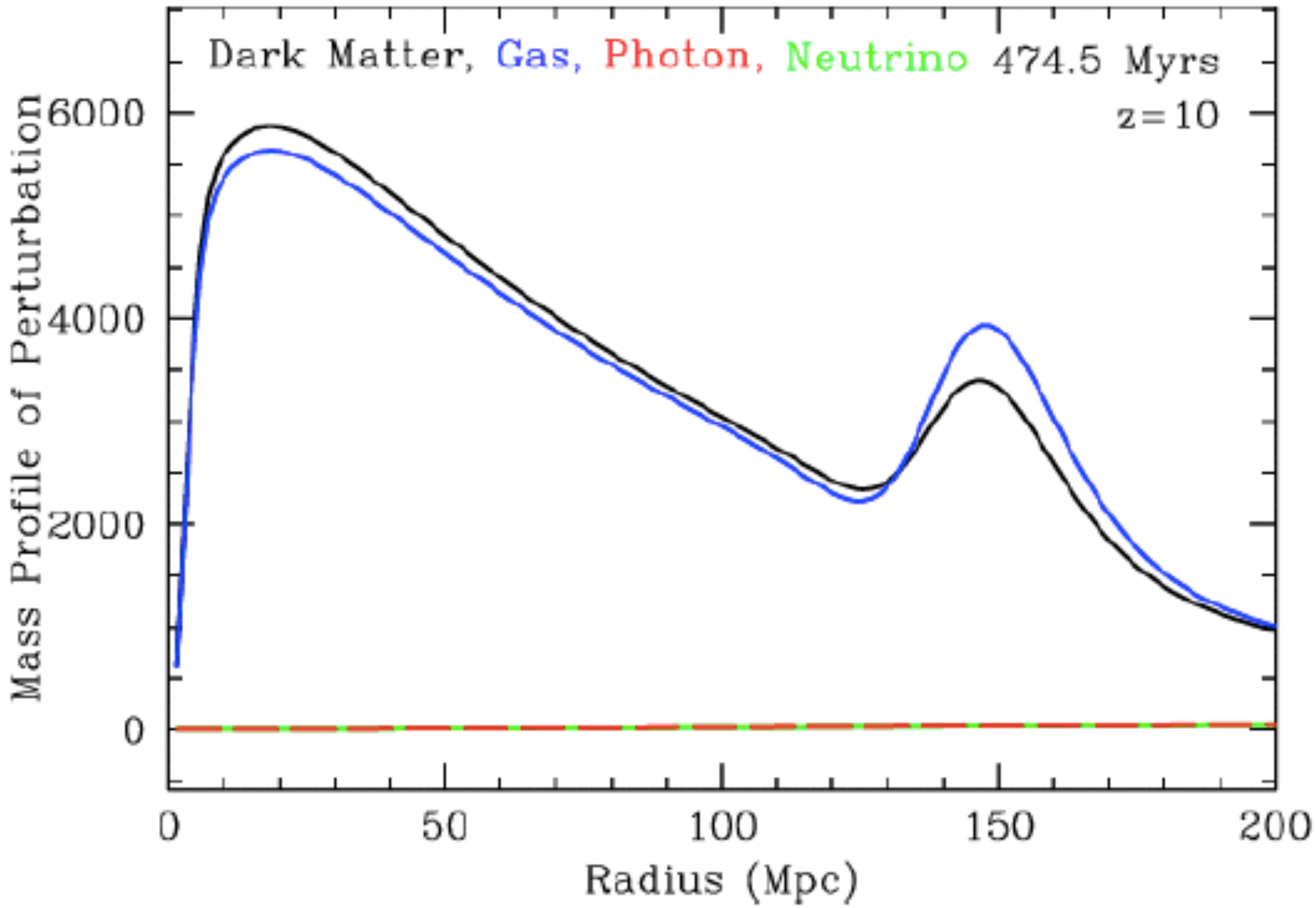

Animation by Daniel Eisenstein

- Massive 'bump' at the centre + spherical shell at $r \sim 150$ Mpc
- Width of shell related to Silk scale

Physics of BAO: individual perturbation

We study the evolution of the density around a single initial perturbation → A shell of matter will form around the initial perturbation

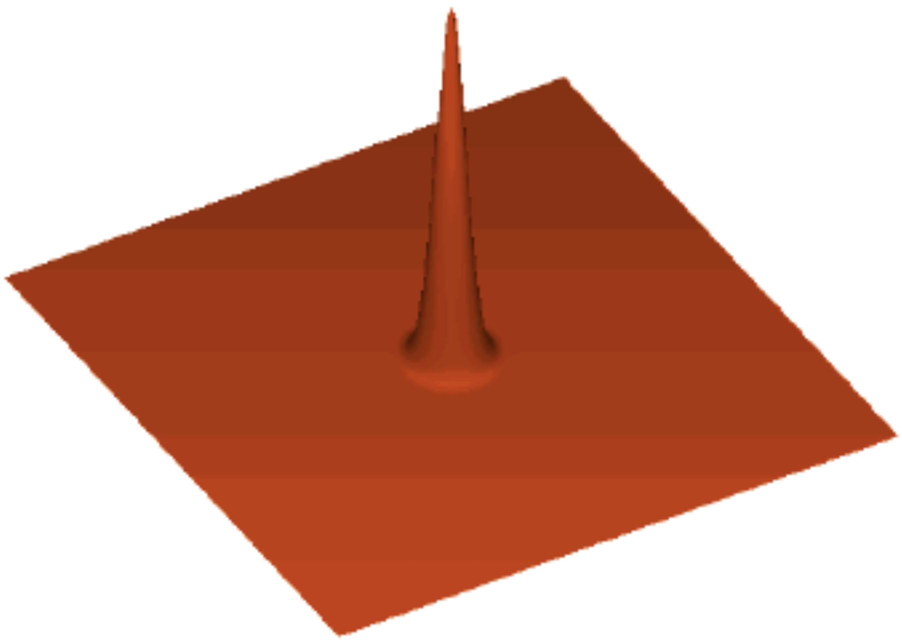

⇒

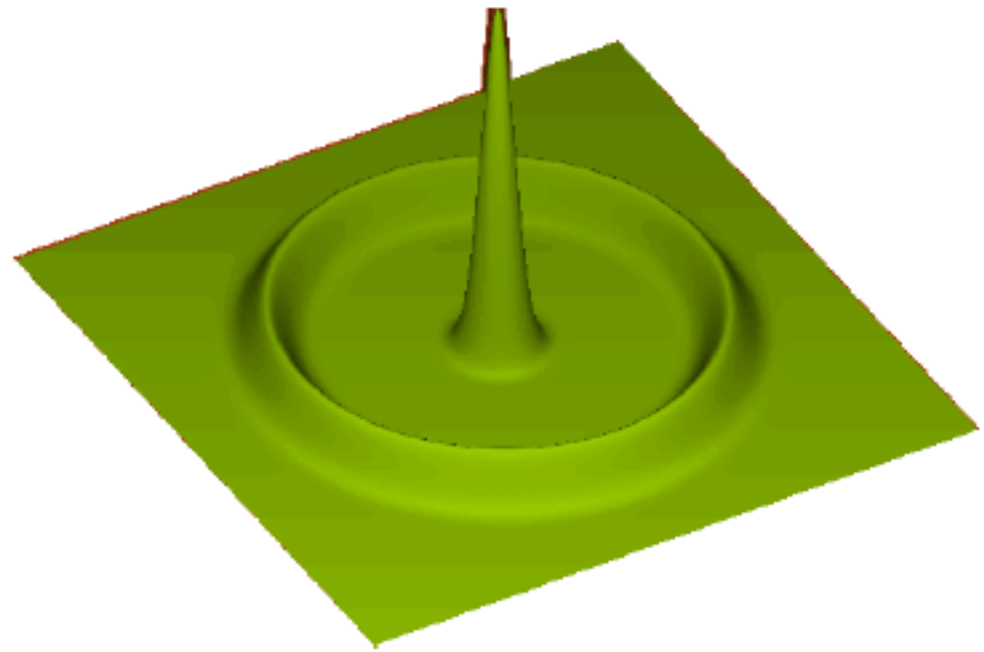

Images from D. Eisenstein's webpage:

Physics of BAO: Galaxy Distribution

Average over all the perturbations. . .

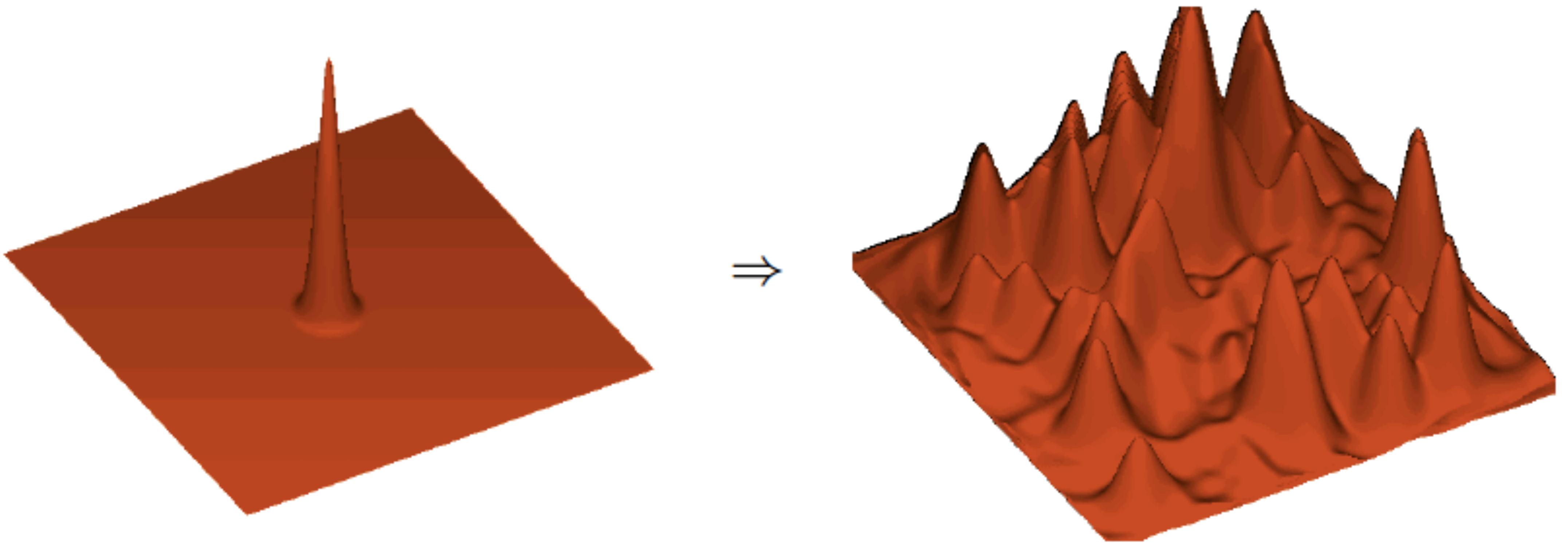

Image from Daniel Eisenstein

Physics of BAO: Cosmic Microwave Background

Evolution of matter profile from a central perturbation before recombination

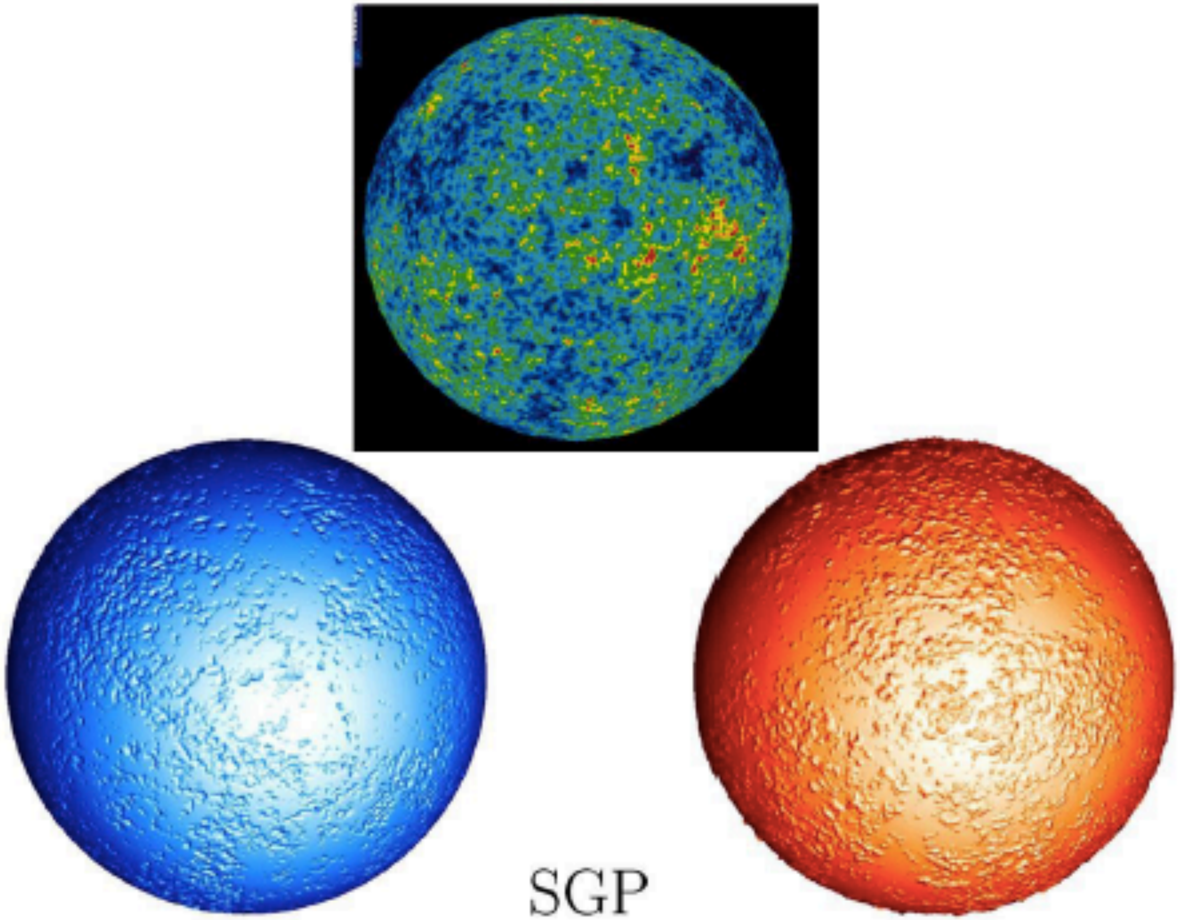

Baryon Acoustic Oscillations detected in the anisotropies of the CMB

Physics of BAO: Cosmic Microwave Background

Evolution of matter profile from a central perturbation before recombination

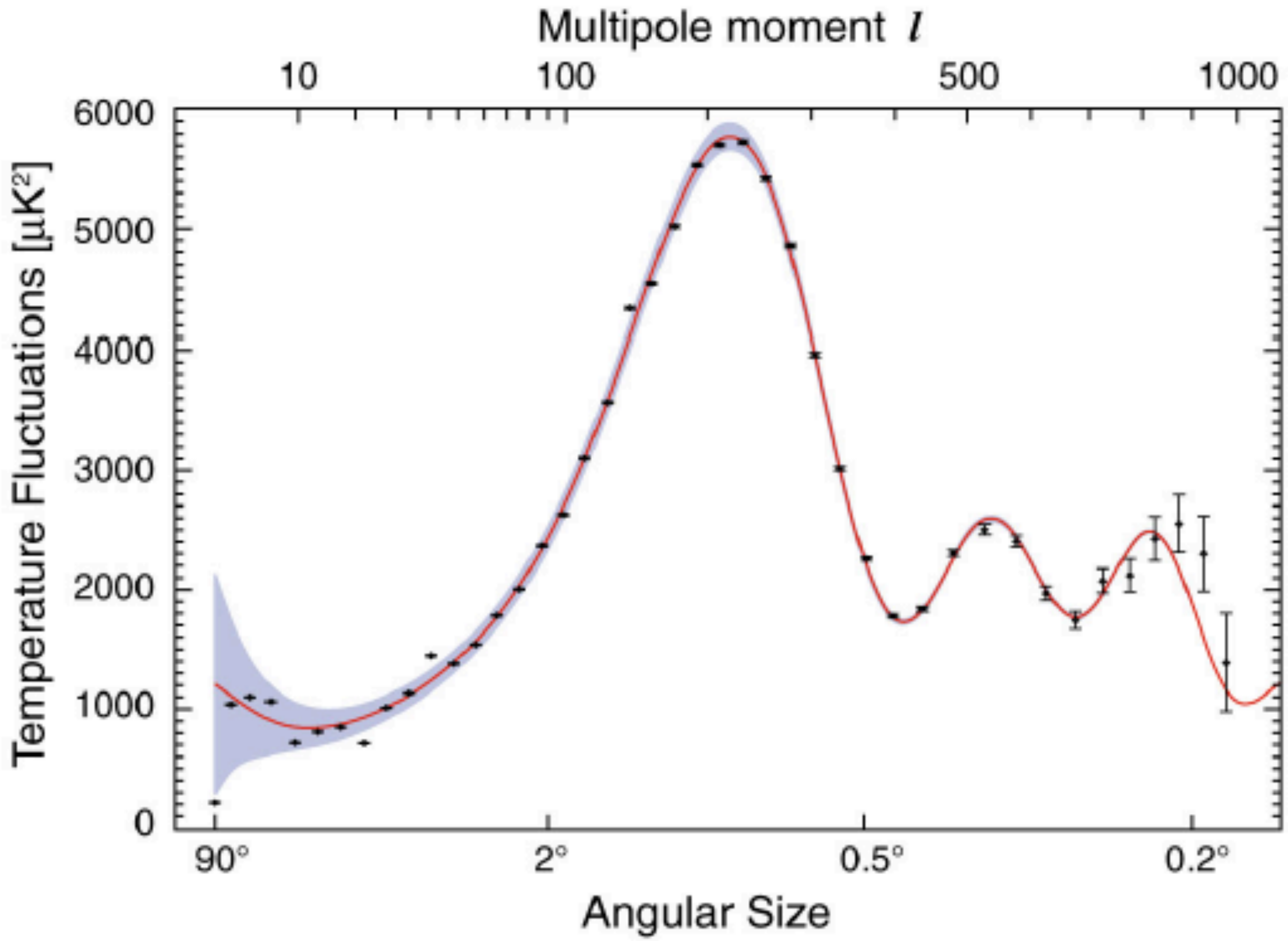

Courtesy of the WMAP science team

Baryon Acoustic Oscillations detected in the anisotropies of the CMB

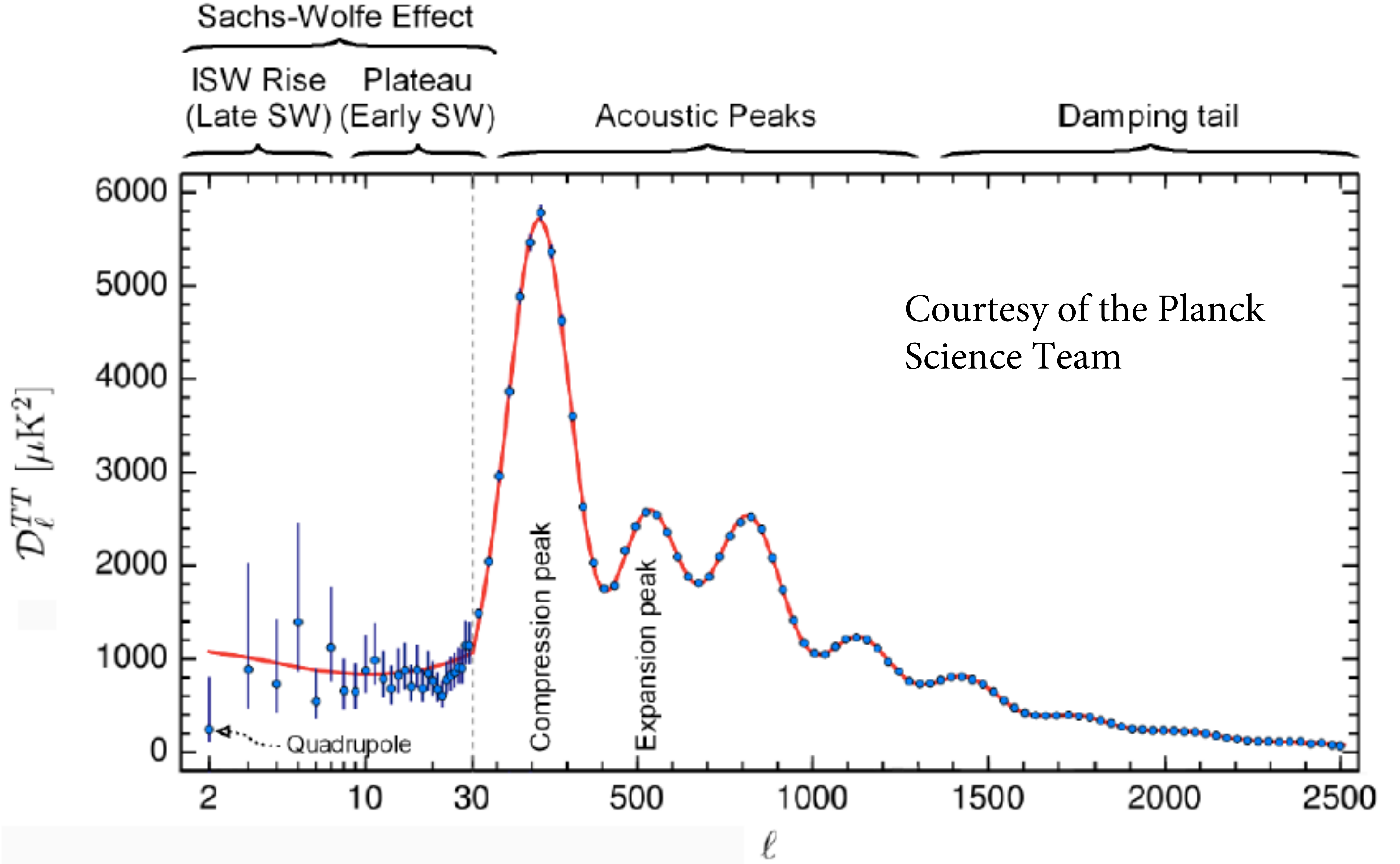
Sachs-Wolfe Effect
ISW Rise
(Late SW)
Plateau
(Early SW)
Acoustic Peaks
Damping tail
6000
5000
4000
3000
2000
1000
0
$\mathcal{D}_\ell^{TT}$ [μK^2]
Courtesy of the Planck
Science Team
Compression peak
Expansion peak
Quadrupole
2
10
30
500
1000
1500
2000
2500
ℓ

Image Credit: E.M. Huff, the SDSS-III team, and the South Pole Telescope Team.
Graphic by Zosia Rostomian

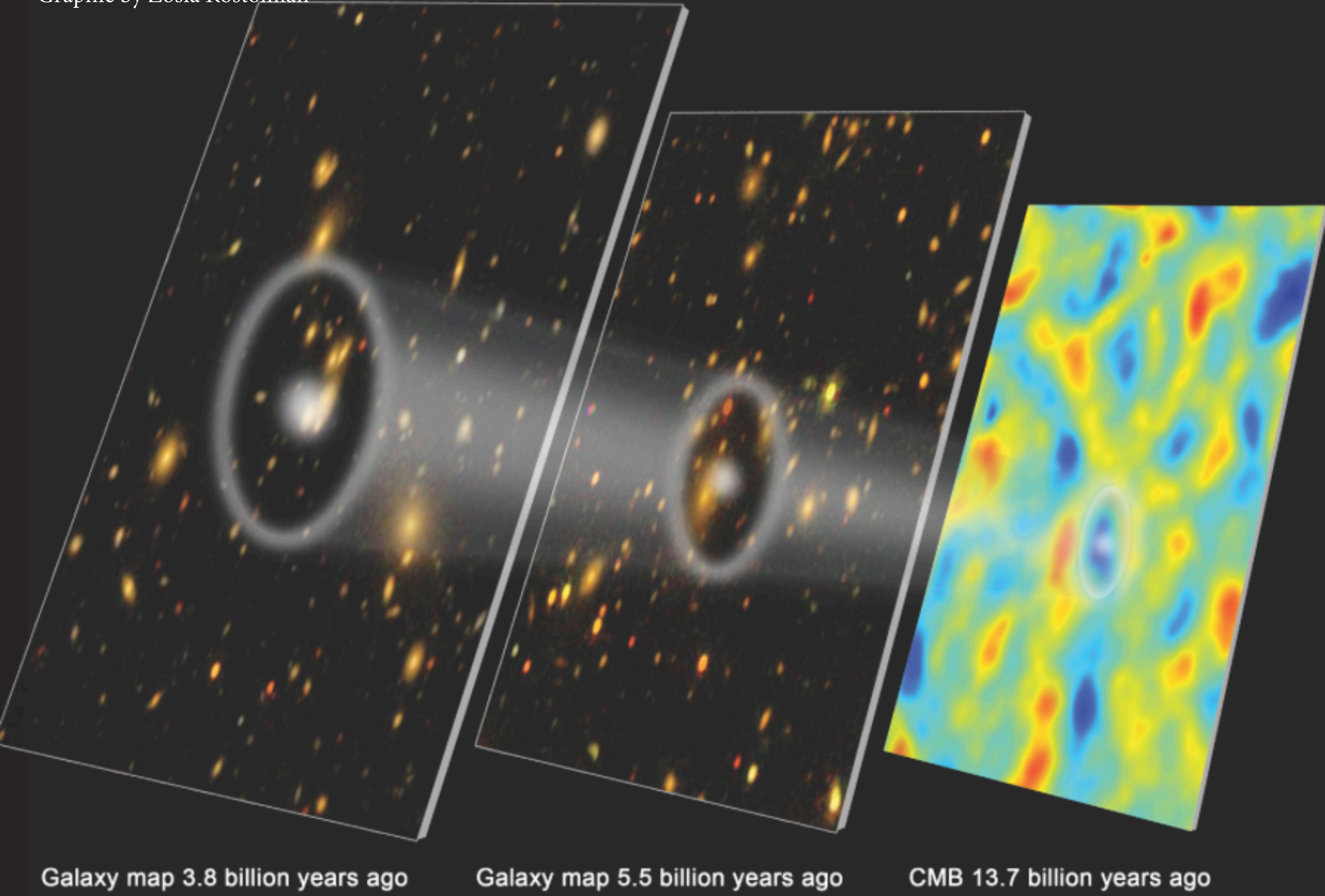

BAO in $\xi(r)$ and $P(k)$

The BAO produce a peak in the correlation function $\equiv$ a series of oscillations in the power spectrum

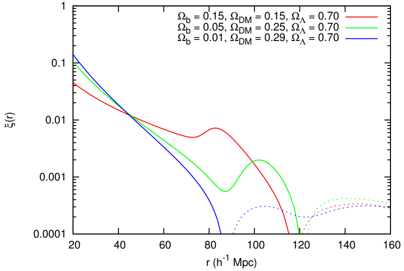

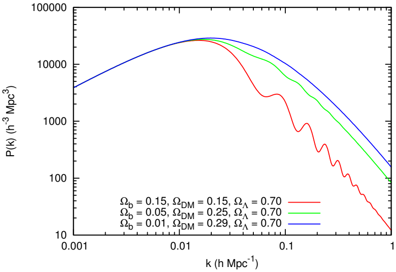

- The characteristic scale in $\xi(r)$ or $P(k)$ (r_s) can be used as a "standard ruler" to constrain the geometry of the universe
- First detected (Eisenstein et al., 2005) in the $\xi(r)$ of SDSS-LRG-DR3 and (Cole et al., 2005) in $P(k)$ of 2dFGRS

Measuring the Geometry of the Universe

- BAO gives us a standard distance with a fixed comoving value (sound horizon at recombination):
  $r_{\mathrm{BAO}} = 153.3 \pm 2.0\,\mathrm{Mpc}$ (WMAP5)
- It can be used as a 'ruler' to measure the geometry of the Universe. For a flat Universe:
  - Radial: $\mathrm{d}r(z) = \frac{c}{H(z)}\mathrm{d}z \rightarrow \Delta z_{\mathrm{BAO}} = H(z) r_{\mathrm{BAO}}$
  - Angular: $d_A(z) = \frac{c}{1+z}\int_0^z \frac{\mathrm{d}z'}{H(z')} \rightarrow \Delta\theta_{\mathrm{BAO}} = \frac{r_{\mathrm{BAO}}}{d_A(z)}$
- Usually constraint a combination of $H(z)$ and $d_A(z)$

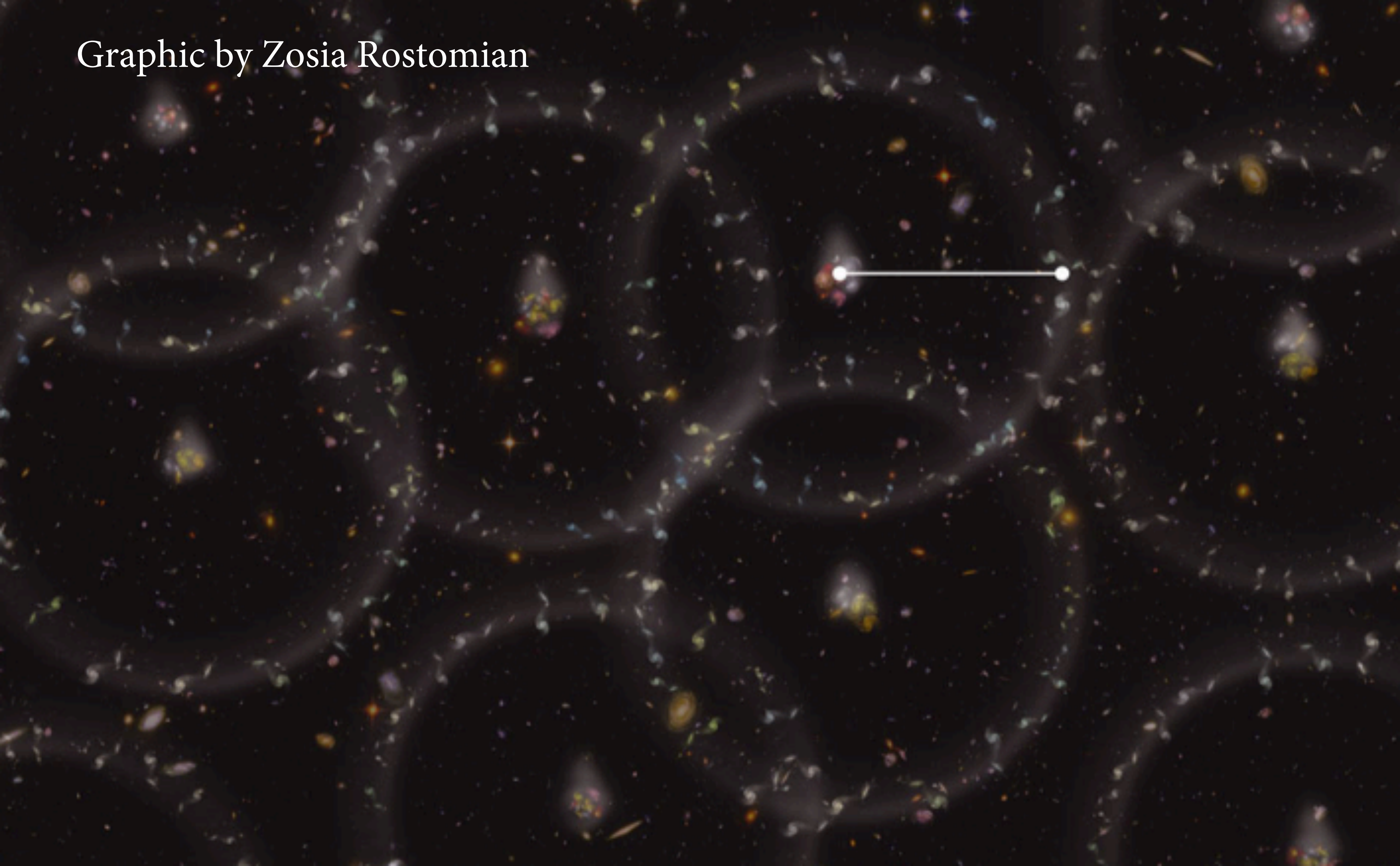

Graphic by Zosia Rostomian

BAO detection in SDSS

First detected (3.5σ) in the $\xi(r)$ of the Luminous Red Galaxies sample of SDSS [Eisenstein et al. (2005)]

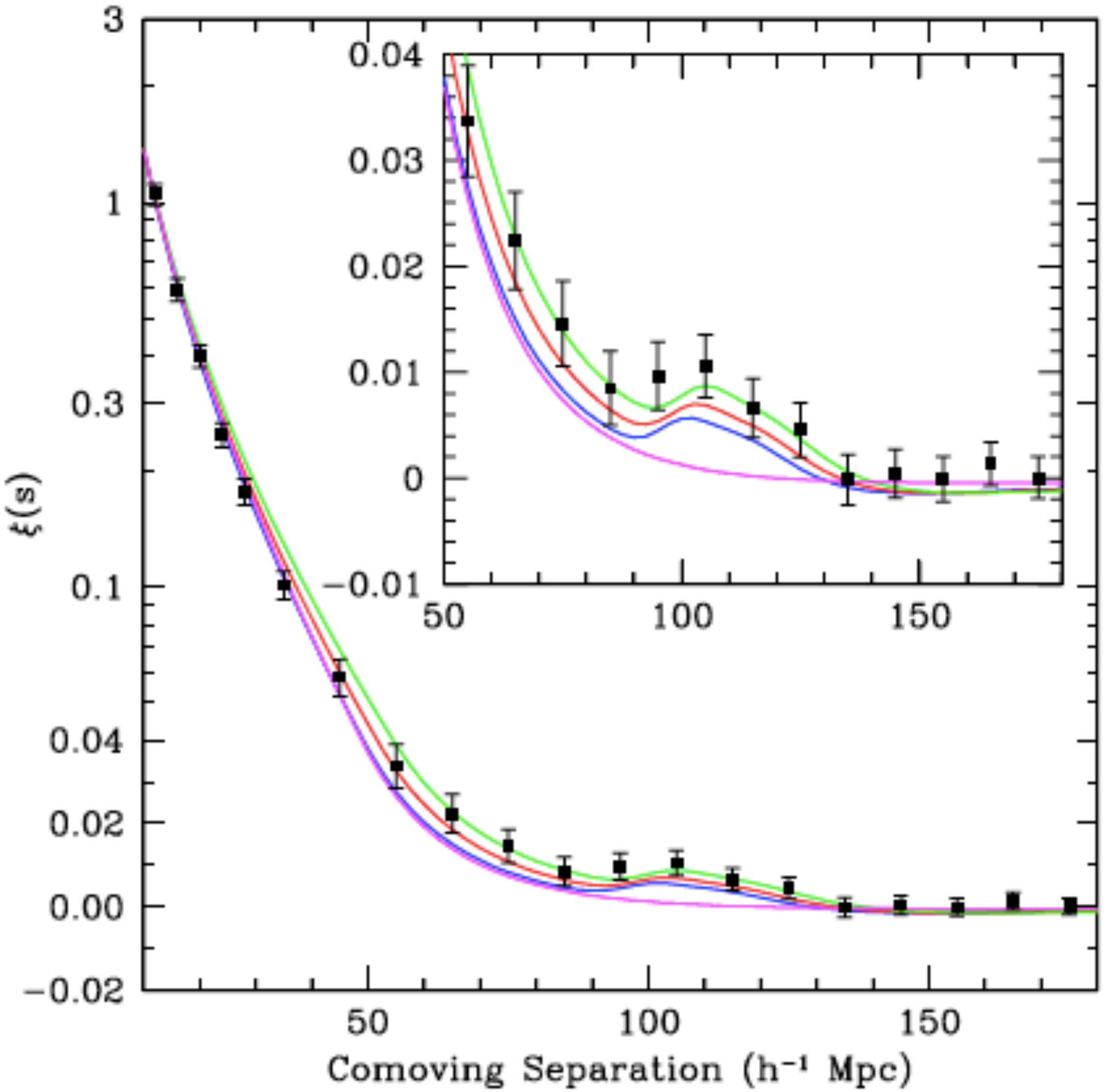

- Confirmed in 2dF and SDSS-photometric at $\sim 2.5\sigma$
- With lower significance in cluster samples

LRG samples

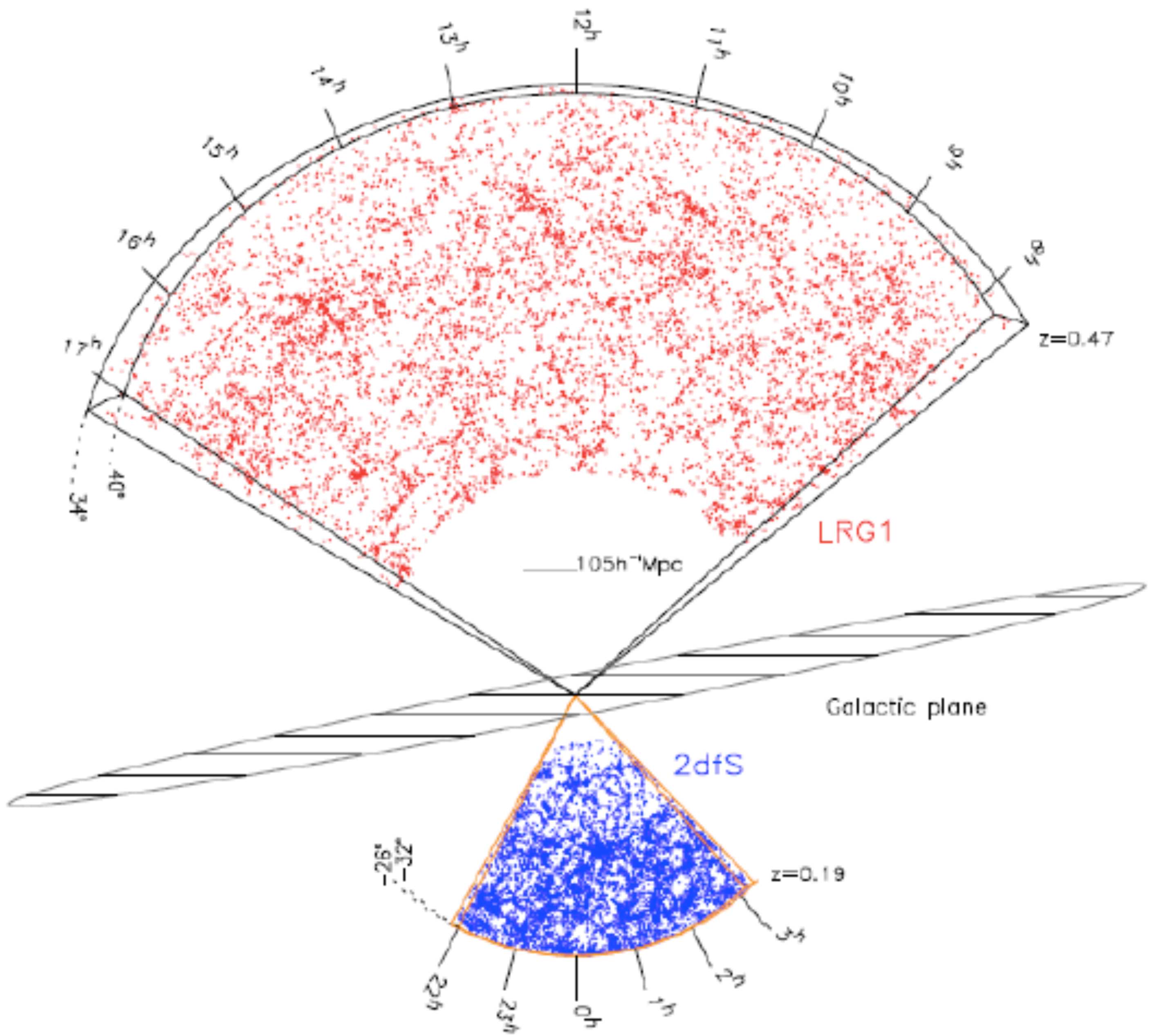

12h
13h
11h
14h
10h
15h
9h
16h
8h
17h
z=0.47
34°
40°
LRG1
105h⁻¹Mpc
Galactic plane
2dfS
-26°
-32°
z=0.19
3h
2h
1h
0h
23h
22h

Correlation function study: samples used

- Aim: to check reliability of BAO detection in $\xi(r)$ by comparing different samples
- Use largest survey to date (SDSS-LRG, DR7) and 2dFGRS $\rightarrow$ complementary samples (in terms of density, z, galaxy properties, etc.)

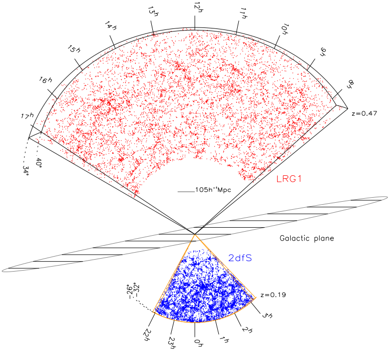

Sample	N	Absolute magnitude	z	Ω (sr)	V ($h^{-3}\mathrm{Gpc}^3$)	$\bar{n}$ (h^3 Mpc^{-3})
DR7-LRG	92,219	$-23.2 < M_g^{0.3} < -21.2$	[0.16, 0.47]	2.02	1.30	7.1×10^{-5}
DR7-LRG-VL	41,195	$-23.2 < M_g^{0.3} < -21.6$	[0.16, 0.40]	2.02	0.817	5.0×10^{-5}
2dFVL	32,388	$-21 < M_{b_J} < -20$	[0.03, 0.19]	0.45	0.024	1.4×10^{-3}

Correlation function study: results

- Estimate $\xi(r)$ using Landy-Szalay method, and errors from block-bootstrap of pair distributions
- BAO peak seen in all three samples $\rightarrow$ stable feature of the LSS
- Width of peak larger than expected (and previous results)
- Results confirmed with these and other samples (SDSS-Main, 6dFGS, WiggleZ).

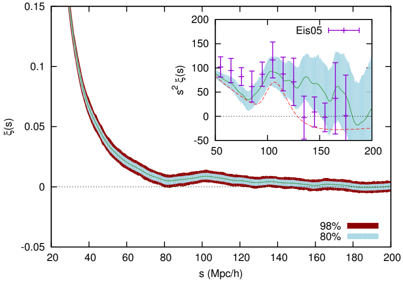

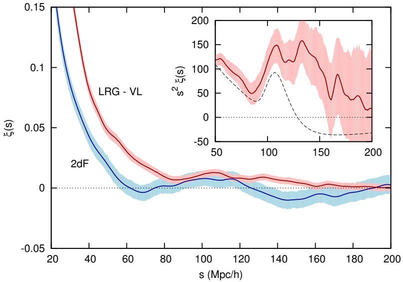

BAO Observational results: cosmological constraints

- Percival et al. 2010

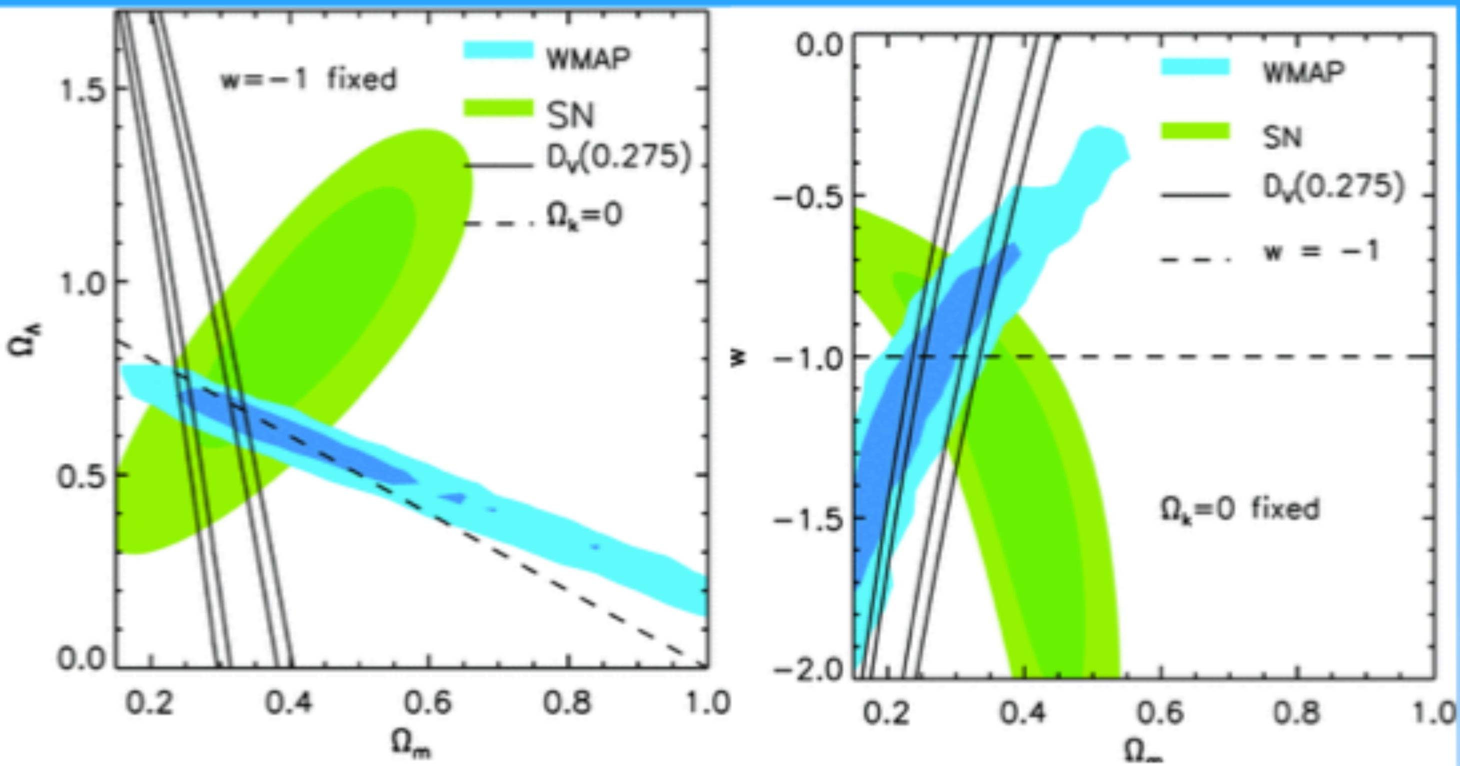

Figure 5. Cosmological constraints on ΛCDM cosmologies (upper panel) and flat CDM models where we allow w to vary (lower panel), from *WMAP5* (blue), Union SN (green) and our constraint on $r_s/D_V(0.275)$ (solid contours). Contours are plotted for $-2\ln\mathcal{L}/\mathcal{L}_{\rm true} < 2.3,\ 6.0$, corresponding to 68 and 95 per cent confidence intervals. The dashed lines show flat models (upper panel) and Λ models (lower panel).

Baryon Acoustic Structures reconstruction

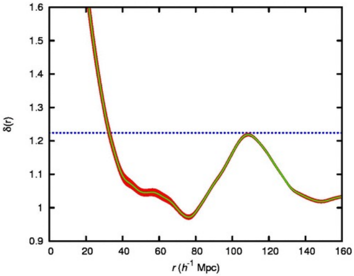

Baryon Acoustic Structures reconstruction

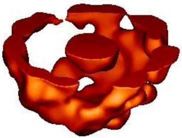

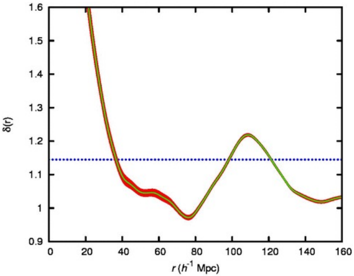

Baryon Acoustic Structures reconstruction

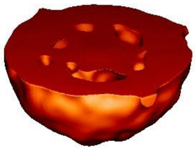

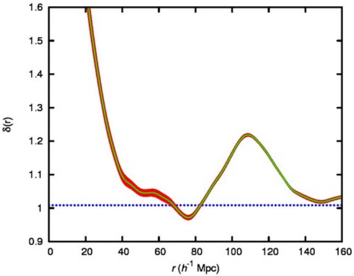

- We recover the 3D shape of the BAO structures $\Rightarrow$ bump at the centre + spherical shell
- From the radial profile we obtain the radius of the shell, $r_{\text{shell}} = 109.5 \pm 3.9\, h^{-1}$ Mpc $\rightarrow$ acoustic scale

Measuring $\xi(r)$ in photometric redshift surveys

- Large Δz in 'photo-z' catalogues $\longrightarrow$ large uncertainties in position (along line of sight) $\longrightarrow$ can not measure $\xi(r)$ directly
- Similar problem to redshift-space effects (e.g. finger-of-God) in 'spectro-z' catalogues (but larger effect for 'photo-z')

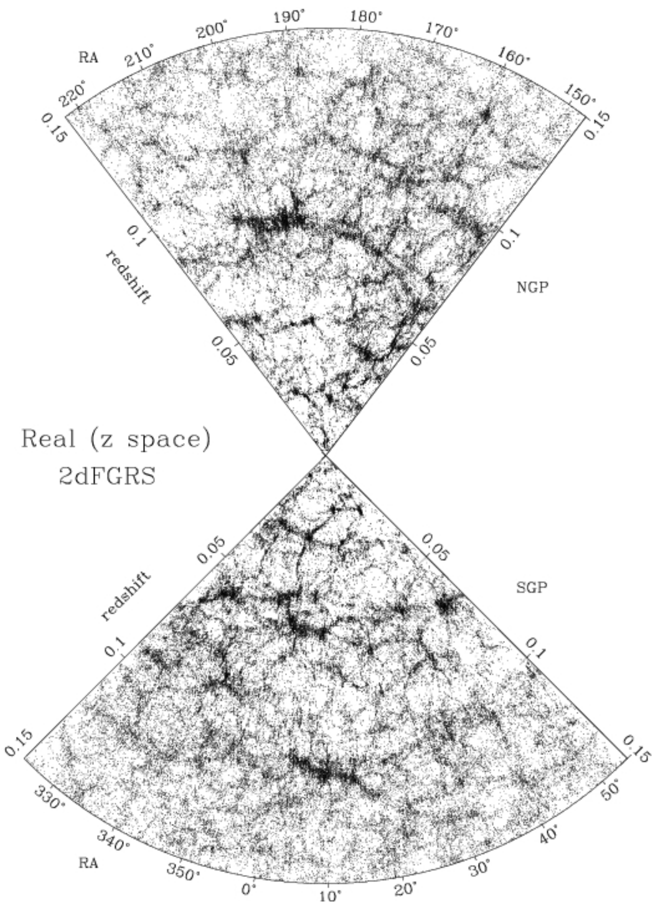

J. Peacock, JENAM 2004

- In 'spectro-z' surveys, the projected correlation function method[4] is used to recover $\xi(r)$

$\Downarrow$

Can we use that method for 'photo-z' catalogues?

[4] Davis&Peebles, ApJ **267**, 465 (1983)

Data: light-cone haloes simulation.

Use the DM halo catalogue from the light-cone simulation of Heinämäki et al. (2005) (astro-ph/0507197)

- Simulation covers $2^\circ \times 0.5^\circ$ in the sky, standard ΛCDM cosmology
- Study restricted to the redshift bin $z \in [2, 3]$
- Geometry of the volume considered: 864 (line-of-sight) $\times 160 \times 40$ (transverse) $h^{-1}\,$Mpc
- Total volume: $4.56 \times 10^6\, h^{-3}\,\mathrm{Mpc}^3$, $\sim 180,000$ haloes

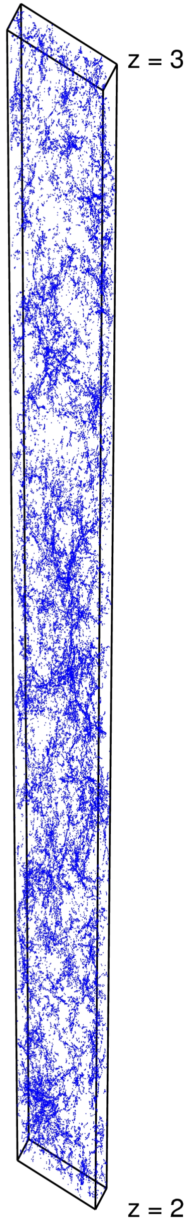

Mock photometric redshift catalogues.

- Simulated photometric redshift catalogues shifting randomly the (redshift-space) position of haloes along the line-of-sight direction
- We assume Gaussian redshift errors, with $\Delta z/(1+z)$ constant for each catalogue $\rightarrow$ valid assumption for 'good' photo-z
- Simulated three 'typical' cases:
  - $\Delta z = 0.05(1+z)$ $\rightarrow$ 'classical' broad-band filter survey
  - $\Delta z = 0.015(1+z)$ $\rightarrow$ 'good' redshifts with ALHAMBRA
  - $\Delta z = 0.005(1+z)$ $\rightarrow$ possible future survey (similar to PAU Survey [5])

[5] Benítez et al. (astro-ph/0807.0535)

Mock photometric redshift catalogues.

- Effect of Δz: projection of the different catalogues on a longitudinal plane

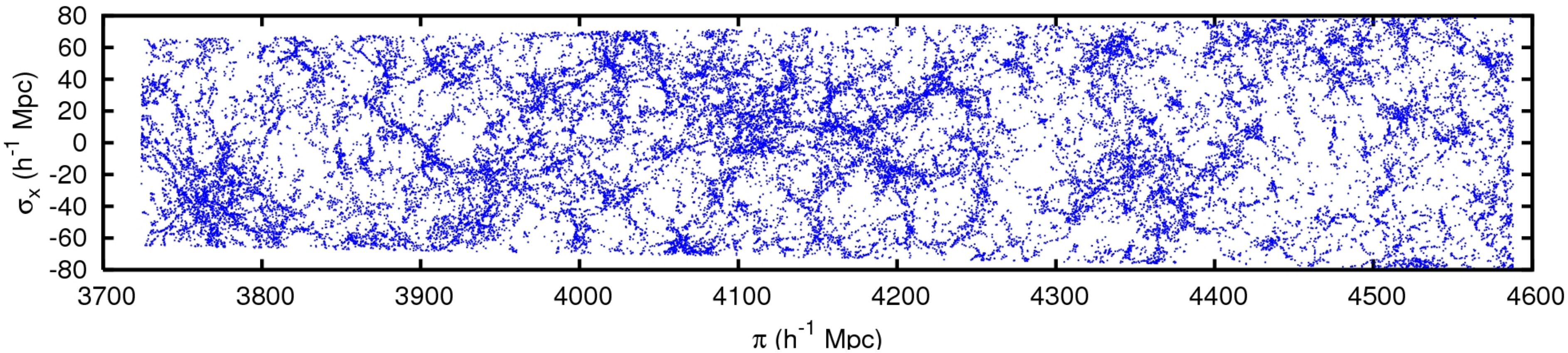

Real-space catalogue

Mock photometric redshift catalogues.

- Effect of Δz: projection of the different catalogues on a longitudinal plane

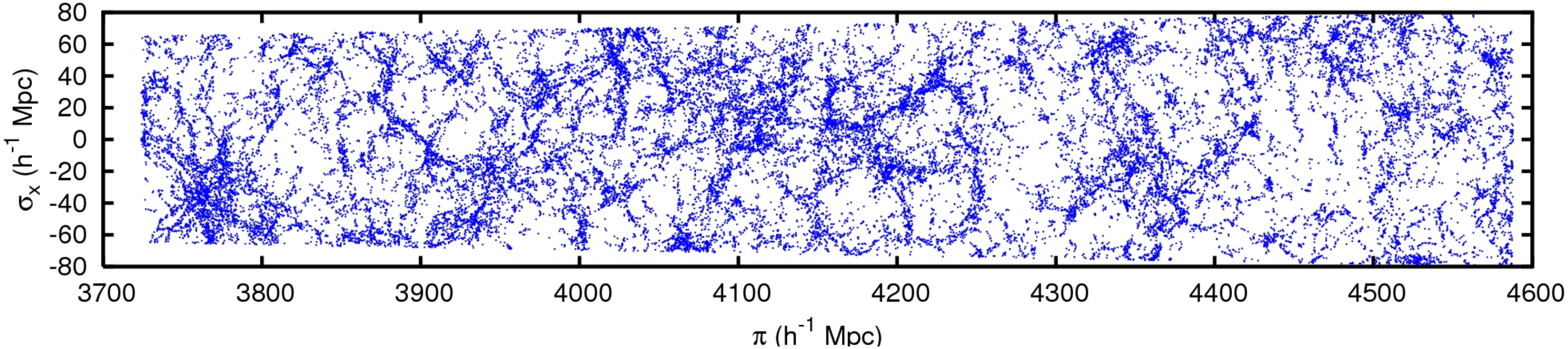

Redshift space

Mock photometric redshift catalogues.

- Effect of Δz: projection of the different catalogues on a longitudinal plane

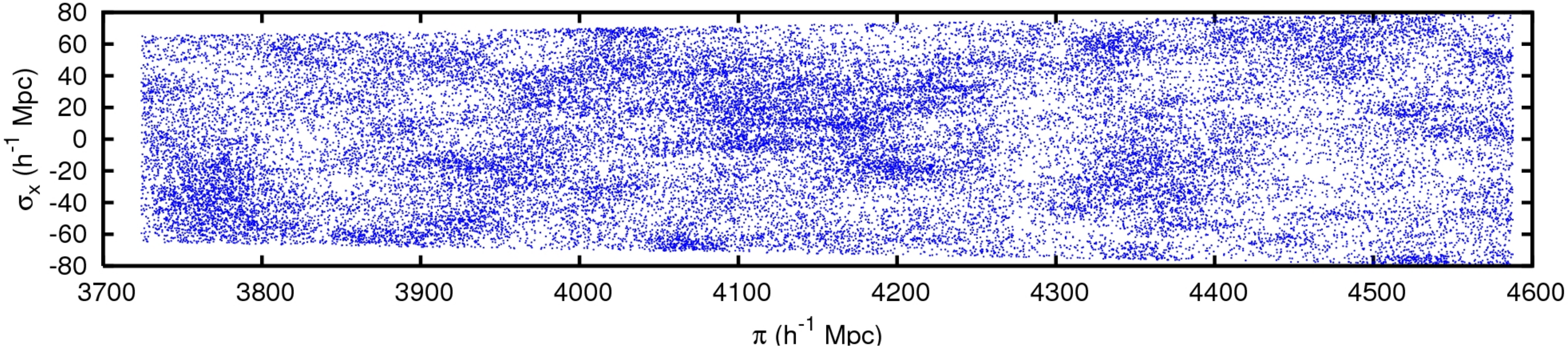

$\Delta z = 0.005(1+z)$ mock catalogue

Mock photometric redshift catalogues.

- Effect of Δz: projection of the different catalogues on a longitudinal plane

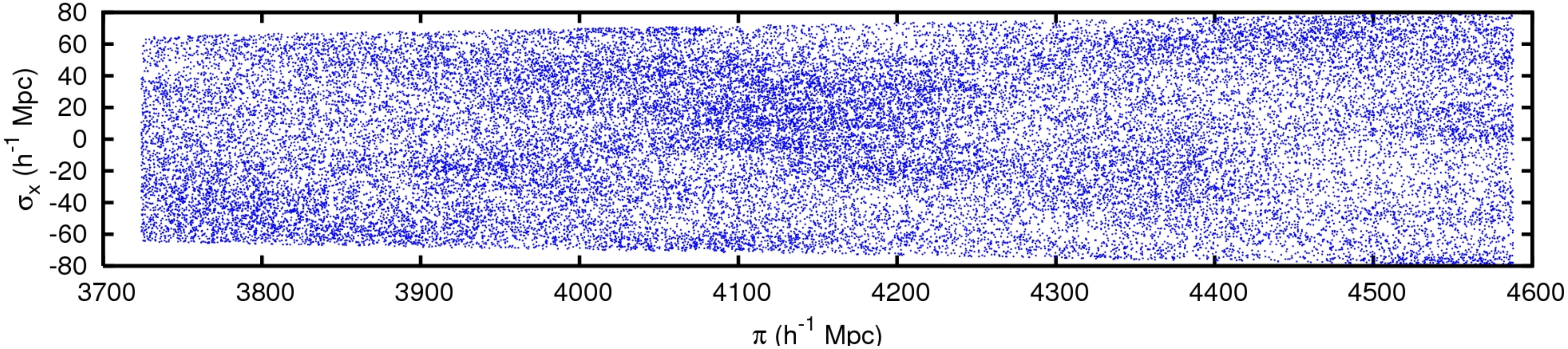

$\Delta z = 0.015(1+z)$ mock catalogue

Mock photometric redshift catalogues.

- Effect of Δz: projection of the different catalogues on a longitudinal plane

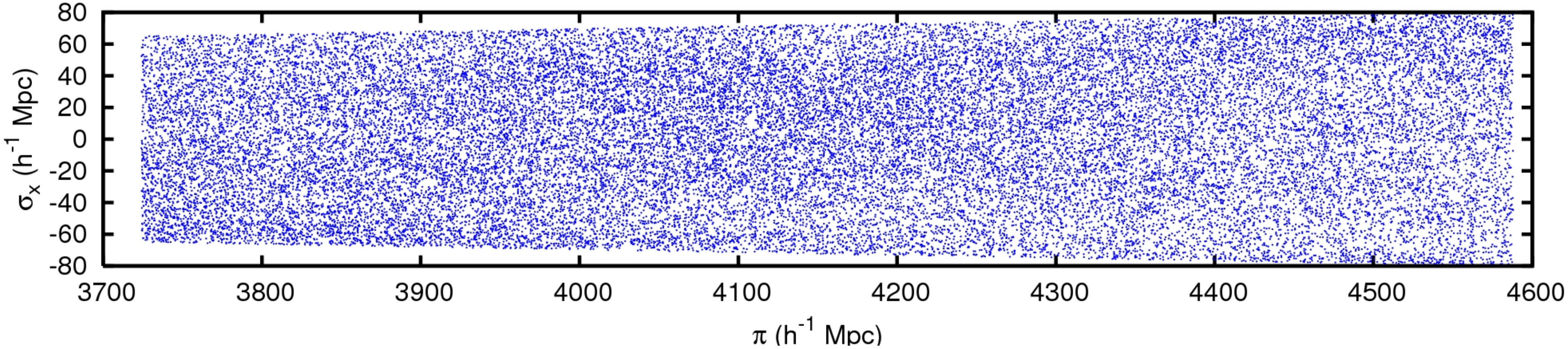

$\Delta z = 0.05(1+z)$ mock catalogue

Decomposition of distances and two-dimensional ξ

- Decompose distances between pairs of galaxies in transverse (σ) and line-of-sight (π).

$$\pi \equiv \frac{|\mathbf{s} \cdot \mathbf{l}|}{|\mathbf{l}|} \quad , \quad \sigma \equiv \sqrt{\mathbf{s} \cdot \mathbf{s} - \pi^2}$$

- Can calculate 'two-dimensional' $\xi(\sigma, \pi) \rightarrow$ count pairs in σ, π bins, and use Landy-Szalay estimator

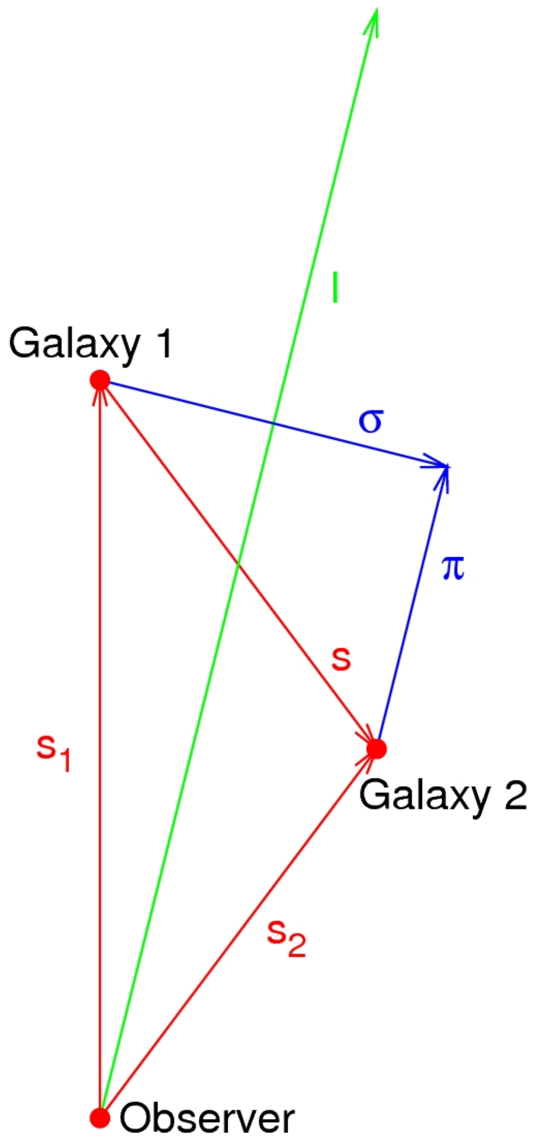

Projected correlation function

- Integrate $\xi(\sigma, \pi)$ along $\pi \to$ 'projected correlation function':

$$\Xi(\sigma) = 2\int_0^\infty \xi(\sigma, \pi)\mathrm{d}\pi$$

- Small angles $\to$ σ not affected by $\Delta z \to \Xi$ not affected by Δz
- Have to choose $\pi_{\max}$ for integration $\to$ optimal value $\pi_{\max} \simeq 4\Delta z$

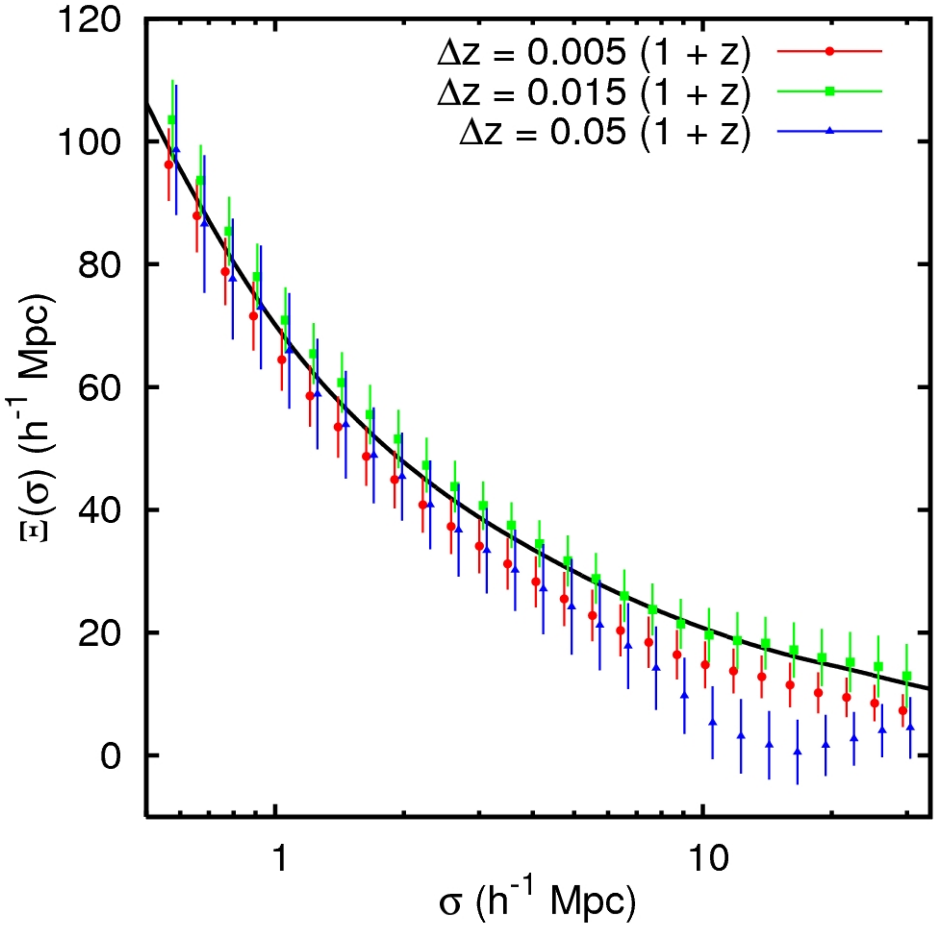

Relation to obtain $\xi(r)$

- Assuming that the (real-space) distribution of galaxies is isotropic $\longrightarrow$ integral relation between $\Xi(\sigma)$ and $\xi_r(r)$

$$\Xi(\sigma) = 2\int_{\sigma}^{\infty} \xi_r(r) \frac{r\mathrm{d}r}{\left(r^2 - \sigma^2\right)^{1/2}}$$

- Inverting the relation $\longrightarrow$ obtain $\xi_r(r)$ in terms of $\Xi(\sigma)$:

$$\xi_r(r) = -\frac{1}{\pi}\int_{r}^{\infty} \frac{\mathrm{d}\Xi(\sigma)}{\mathrm{d}\sigma} \frac{\mathrm{d}\sigma}{\left(\sigma^2 - r^2\right)^{1/2}}$$

$$\downarrow$$

Can obtain $\xi_r(r)$ by numerical integration of $\Xi(\sigma)$

- Have to choose a σ_{max} for integration $\longrightarrow$ given by survey geometry

Why so many filters?

Number of filters vs Accuracy

Benítez et al. 2009

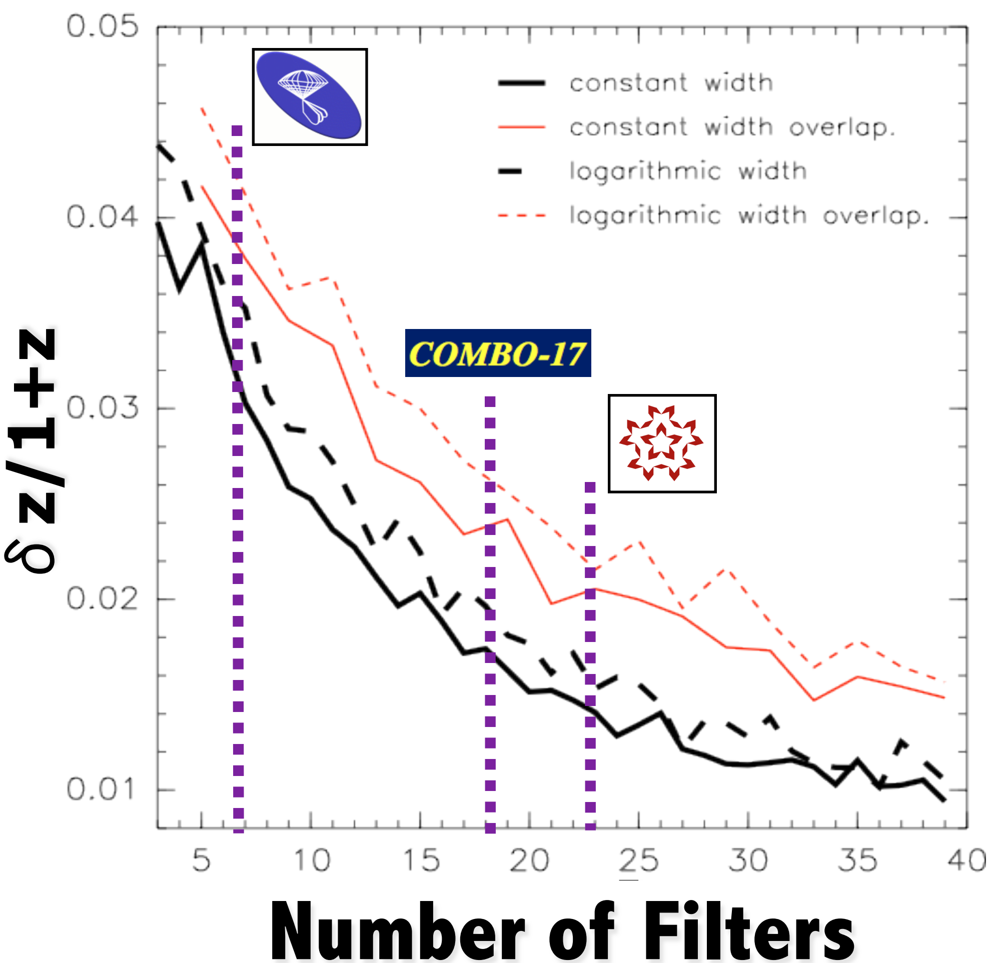

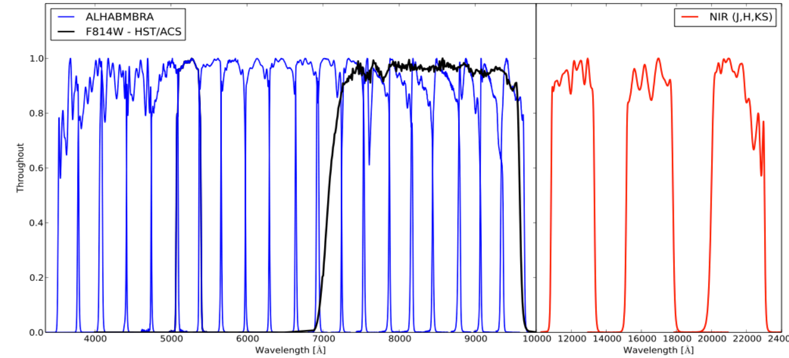

Photometric Redshift surveys

survey	Reference	Bands	$\delta_z/(1+z)$
HDF	Sawicki (1997)	4	0.080
SDSS/DR6	Csabai (2003)	5	0.035
SWIRE	Rowan-Robinson (2008)	5	0.035
HUDF	Coe (2006)	6	0.040
HDF	Fernández-Soto (1999)	7	0.060
CFHTLS	Ilbert (2006)	9	0.030
GOODS	Dahlen (2010)	12	0.040
CLASH	Molino (2013, prep.)	16	0.025
COMBO-17	Wolf (2004)	17	0.020
ALHAMBRA	Molino (this work)	23	0.013
COSMOS	Ilbert (2009)	30	0.007
MUSYC	Cardamone (2010)	32	0.007
JPAS	Benítez (2009a, 2013, prep.)	59	0.003

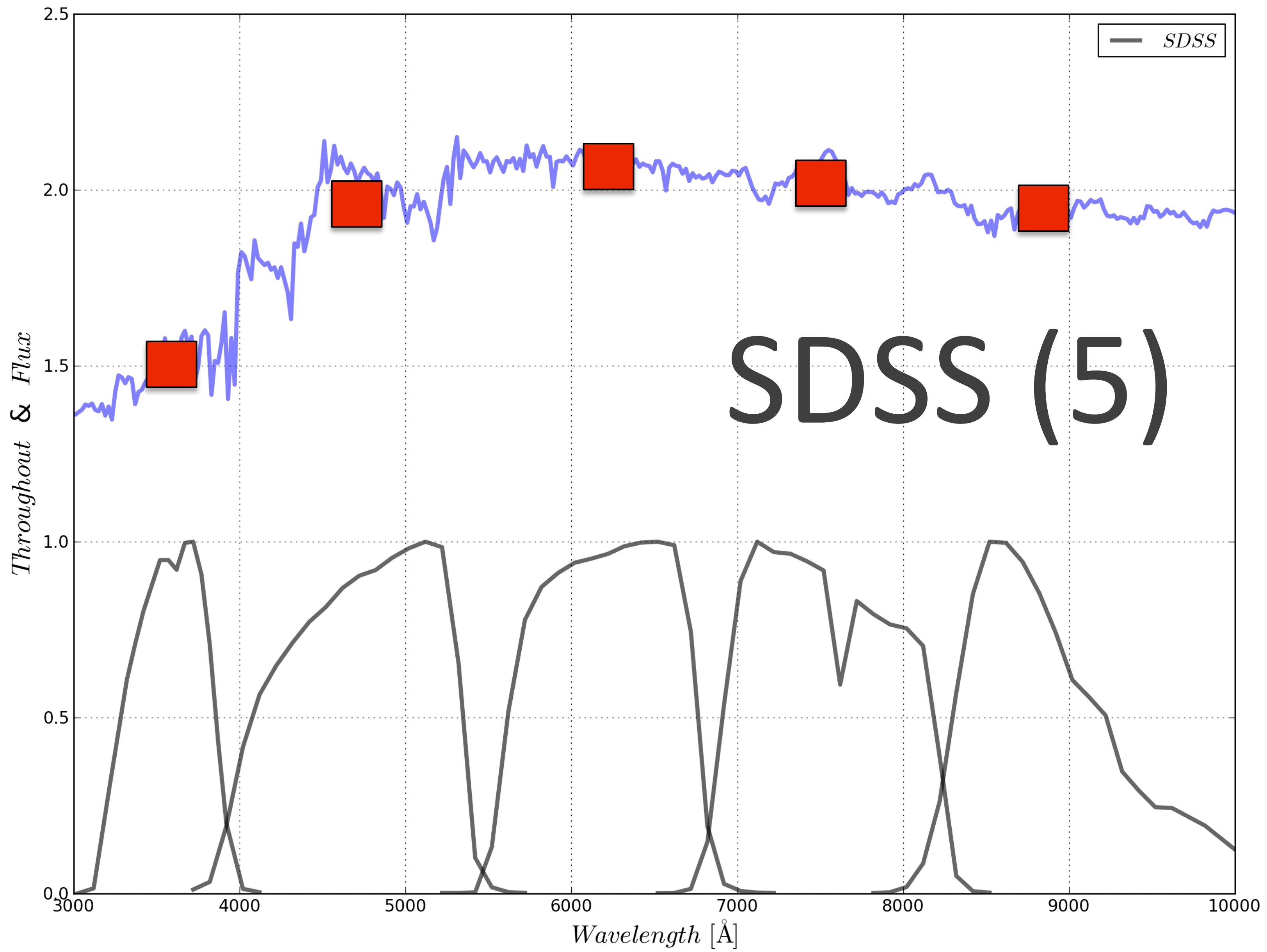

SDSS (5)
SDSS
Throughout & Flux
Wavelength [Å]
0.0
0.5
1.0
1.5
2.0
2.5
3000
4000
5000
6000
7000
8000
9000
10000

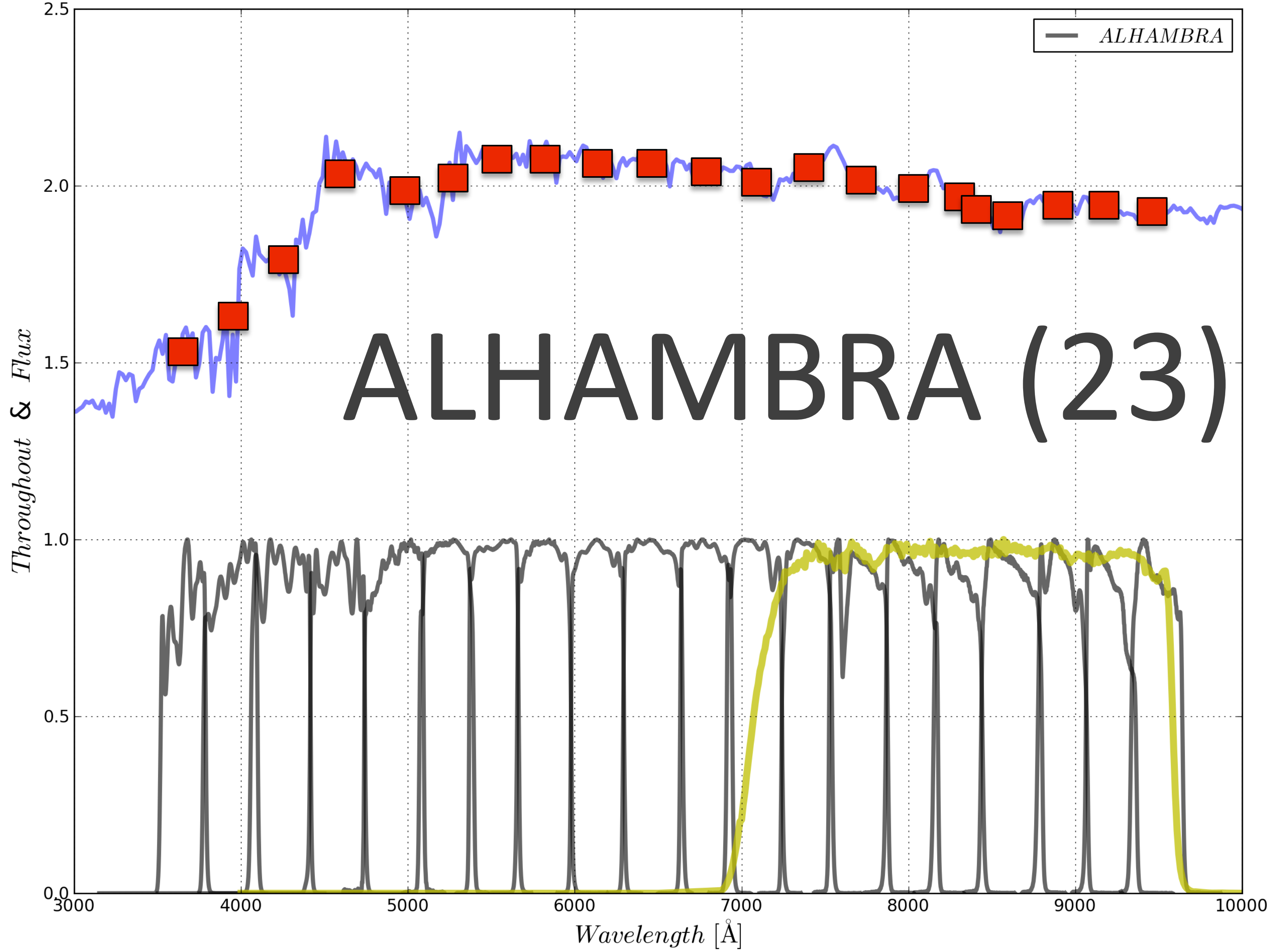

ALHAMBRA
ALHAMBRA (23)
2.5
2.0
1.5
1.0
0.5
0.0
Throughout & Flux
3000
4000
5000
6000
7000
8000
9000
10000
Wavelength [Å]

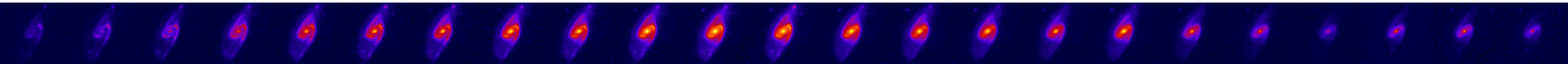

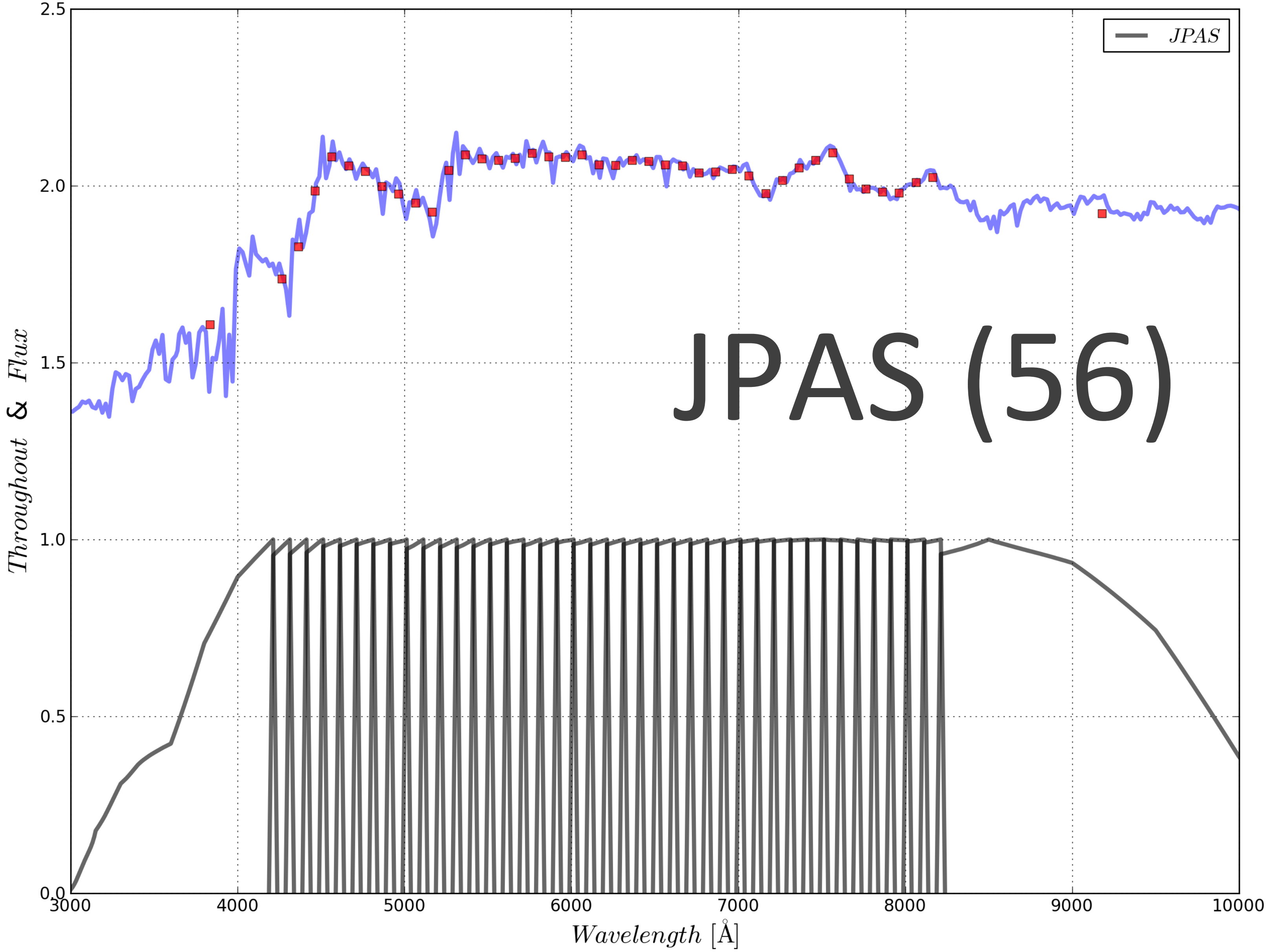
JPAS (56)
JPAS
Throughout & Flux
Wavelength [Å]
2.5
2.0
1.5
1.0
0.5
0.0
3000
4000
5000
6000
7000
8000
9000
10000

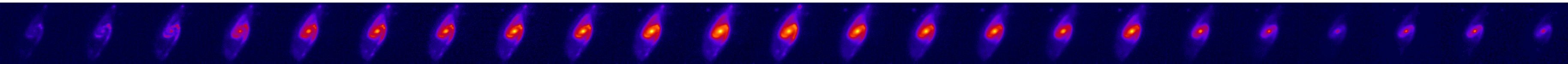

Large scales again
BAO form photometric
redshift surveys

Distortions for expected photometric surveys

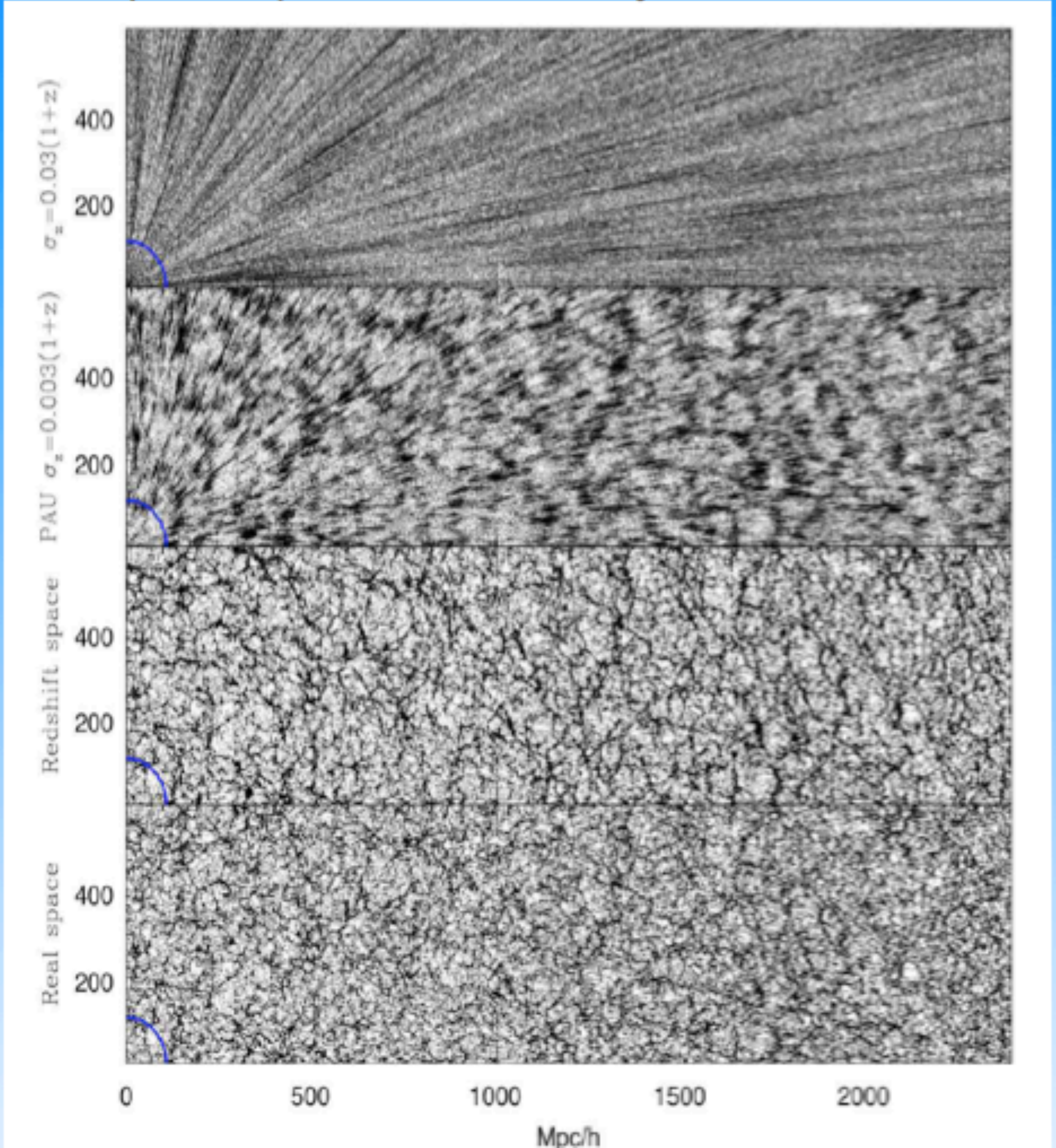

z-space, *Δz* = *0.03(1+z)* + peculiar velocities

z-space, *Δz* = *0.003(1+z)* + peculiar velocities

z-space, perfect z-resolution + peculiar velocities

Real space, perfect resolution

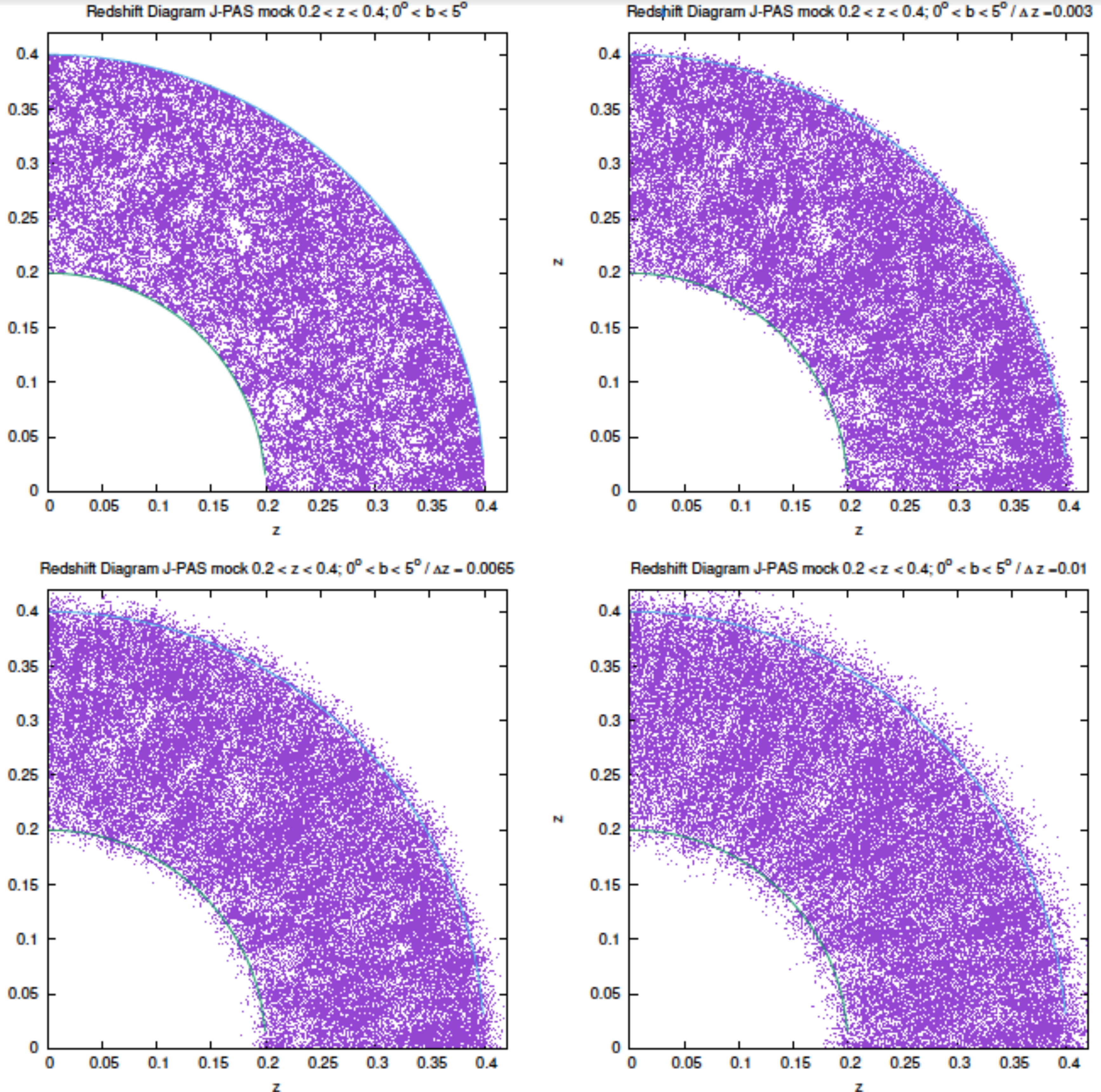
Redshift Diagram J-PAS mock 0.2 < z < 0.4; 0° < b < 5°
Redshift Diagram J-PAS mock 0.2 < z < 0.4; 0° < b < 5° / Δz = 0.003
Redshift Diagram J-PAS mock 0.2 < z < 0.4; 0° < b < 5° / Δz = 0.0065
Redshift Diagram J-PAS mock 0.2 < z < 0.4; 0° < b < 5° / Δz = 0.01
z
z
0
0.05
0.1
0.15
0.2
0.25
0.3
0.35
0.4

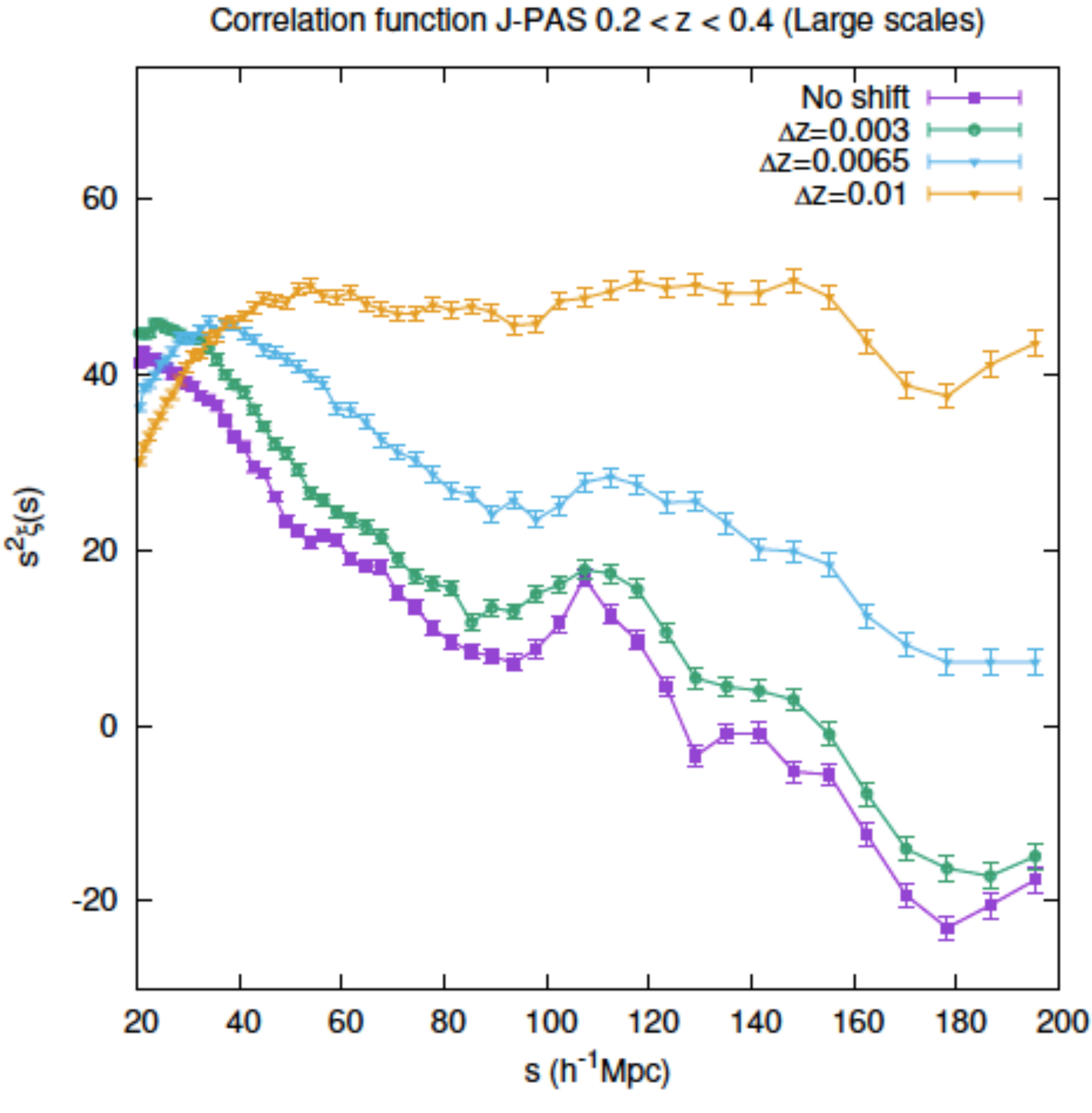
Correlation function J-PAS 0.2 < z < 0.4 (Large scales)
No shift
ΔZ=0.003
ΔZ=0.0065
ΔZ=0.01
60
40
20
0
-20
20
40
60
80
100
120
140
160
180
200
$s^2\xi(s)$
s (h^{-1}Mpc)

Observatori Astronòmic
Universitat de València

www.uv.es/martinez

Muchas Gracias

Vicent.Martinez@uv.es